

Disentangling sensory and top-down information during perceptual decision making

M a s t e r ' s T h e s i s

in partial fulfillment of the requirements for the degree of
Master of Science in Computational Neuroscience

Author:

Paola SUÁREZ
Matriculation Number 386048

Supervisor:

Prof. Dr. Henning SPREKELER

Professor for Modelling of Cognitive Processes
Bernstein Center for Computational Neuroscience Berlin,
Technischne Universität Berlin
and Humboldt-Universität zu Berlin

Berlin, Tuesday 30th July, 2019

Eidesstattliche Versicherung

Hiermit erkläre ich, dass ich die vorliegende Arbeit selbstständig und eigenhändig sowie ohne unerlaubte fremde Hilfe und ausschließlich unter Verwendung der aufgeführten Quellen und Hilfsmittel angefertigt habe.

Statutory Declaration

I declare in lieu of oath that I have written this thesis independently, without illicit assistance from third parties and using solely the aids mentioned.

Berlin, Tuesday 30th July, 2019

Paola SUÁREZ

Acknowledgements

The inspiration for this thesis sits in the hope to bring theory and biology closer. In particular, my interests drove me to questions regarding decision making and perception. After sitting in a park, sharing some food and discussing our interests, Filip Vercruyse and I came out with the main idea of the project. We then received full support from Henning Sprekeler and started the adventure. I am very grateful for their enthusiasm, long discussions and motivation throughout the development of this thesis.

I am also grateful to the Sprekeler Lab in general, for sharing their knowledge and insights in a collaborative atmosphere. And I would like to add a kind comradeship nod to my female peers: Laura, Loreen and Elisabeth, for their kind support in crucial matters regarding cluster setup, proof reading and feedback.

Finally, I thank Matthew Larkum for his support and insightful views on the scope of this work. I thank BCCN professors and my fellow classmates for helping me acquire the tools needed to be a computational neuroscientist. This work was possible thanks to previous support from the Mexican National Council for Science and Technology (Conacyt).

Abstract

In the field of perceptual decision making, the relationship between the activity of sensory neurons and decision outcomes is known as choice probability (CP) and has been extensively studied. A problem regarding CP is that the origin of the variability in neuronal activity and decision outcomes is unclear. Hence, it is difficult to assess whether sensory neurons have a causal effect on upcoming decisions or not. A purely bottom-up approach supports a causal interpretation, in which variability in choices arises from random fluctuations in the response of sensory neurons to external stimuli. On the other hand, a top-down approach supports a non-causal interpretation, and states that variability in choices reflects fluctuations in the influence of cognitive factors (e.g., attentional signals or intrinsic biases) on the activity of sensory neurons. Recently, sustained traces of CP were disentangled into an early, bottom-up component and a late, top-down component through sophisticated computational modeling. However, using an indirect measurement of bottom-up and top-down influences on choice, results in an expensive way to study decision networks under different, more complex conditions. In the present work I will extend a network model for perceptual decision making with two-compartment sensory neurons to create a diverse repertoire of spiking patterns. The theory of multiplexing suggests that sensory neurons use different spiking patterns to transmit information from different streams. Thus, this extension provides a direct method to differentiate between bottom-up and top-down contributions to an upcoming decision. Overall, the present work suggests a biologically plausible, simple and generalizable method to tackle the interpretation problem regarding CP.

Zusammenfassung

Im Bereich der perzeptuellen Entscheidungsfindung ist die Beziehung zwischen der Aktivität der sensorischen Neuronen und den Entscheidungsausgängen auch bekannt als „Choice Probability“ (CP), die umfassend untersucht worden ist. Die Ursprünge der Variabilität in der neuronalen Aktivität und den Verhaltensergebnissen sind jedoch weitgehend unbekannt. Daher ist es schwierig zu beurteilen, ob sensorische Neuronen einen kausalen Einfluss auf anstehende Entscheidungen haben. Ein ausschließlich „Bottom-up“-Ansatz unterstützt eine kausale Interpretation, bei der die Variabilität in den Entscheidungen aus zufälligen Schwankungen in der Reaktion von sensorischen Neuronen auf externe Reize resultiert. Andererseits befürwortet der „Top-Down“-Ansatz, dass kognitive Prozesse wie Aufmerksamkeitssignale und intrinsische Verzerrungen neuronale Aktivitäten beeinflussen und die Schwankungen dieses Einflusses sich in der Varibilität in den Entscheidungen widerspiegeln. Somit schlägt dieser Ansatz eine nicht-kausale Interpretation der CP vor. In jüngster Zeit wurden anhaltende Signale von CP mit Hilfe von ausgefeilten Computermodellen in eine frühe „Bottom-up“-Komponente und eine späte „Top-down“-Komponente aufgeteilt. Die indirekte Messung von „Bottom-up“- und „Top-down“-Einflüssen auf die Entscheidung ist jedoch eine rechnerisch sehr aufwendige Methode und eignet sich nicht für die Untersuchung von komplexen Entscheidungsnetzwerken. In der vorliegenden Arbeit werde ich ein Netzwerkmodell der Entscheidungsfindung um ein Zwei-Kompartiment-Modell für die sensorischen Neuronen erweitern, welches ein umfangreiches Repertoire an Spiking-Muster produziert. Laut der „Multiplexing“-Theorie benutzen sensorischen Neuronen unterschiedliche Spiking-Muster um verschiedenen Informationsströme auseinanderzuhalten. Somit stellt diese Erweiterung eine direkte Methode dar, um zwischen den „Bottom-up“- und „Top-down“-Einflüssen auf eine bevorstehende Entscheidung zu unterscheiden. Die vorliegende Arbeit bietet eine biologisch plausible, einfache und verallgemeinerbare Methode, um das Interpretationsproblem der CP näher zu untersuchen.

Contents

Abstract	vii
1 Introduction to decision making	1
1.1 Perceptual decision making	2
1.1.1 Sensory neuronal activity correlates with choices	3
1.1.2 Sensory neural fluctuations emerge from different origins	4
1.2 Hierarchical network for perceptual decision making	5
1.2.1 Model limitations	7
1.3 Extended hierarchical network	8
1.3.1 Motivation	9
1.3.2 Two-compartment model for sensory pyramidal neurons	10
2 Methods	11
2.1 Hierarchical network	11
2.1.1 Sensory circuit	12
2.1.2 Decision circuit	14
2.1.3 External stimulus	14
2.2 Spike count statistics and choice probability	15
2.3 Burst coding and multiplexing	16
2.4 Simulation details	17
3 Results	19
3.1 Replication of hierarchical network	19
3.2 Hierarchical network with two-compartment sensory neurons	23
3.2.1 Two-compartment sensory neurons affect bottom-up influences on choices	23
3.2.2 Extended hierarchical network models perceptual decisions . .	25
3.3 Decoding top-down influence through a multiplexed neural code . .	27
4 Discussion	33
4.1 Stabilization of hierarchical network with two-compartment sensory neurons	34
4.2 Multiplexing in recurrent networks	35
4.3 Future perspectives	36
Bibliography	39

Chapter 1

Introduction to decision making

Decisions are a hallmark of higher cognition and exert a crucial influence in our lives. The scope of the decision making process is vast and complex: from simple, seemingly unimportant everyday choices to life-changing commitments. In general, a decision emerges from external evidence and the expected cost or value associated with behavioral outcomes (Gold and Shadlen 2007; Resulaj et al. 2009). In order to understand how decisions are formed within our brains, it is crucial to investigate the link between neuronal activity and behavioral choices (Parker and Newsome 1998; Romo et al. 2002).

The first link between sensory neuronal activity of macaque monkeys and behavioral choices was described by Britten et al. (1996), and set a milestone in the field of decision making. In the following decades, experimental results found a robust relationship between the activity of sensory neurons and an animal's choice in a wide variety of perceptual tasks (Nienborg, R. Cohen, and Cumming 2012). A robust relationship in this context means that the activity of a group of neurons is critical to the generation of a behavioral choice. One requirement to assess this claim says that fluctuations in neuronal activity to different presentations of identical external stimuli should be predictive of decision outcomes (Parker and Newsome 1998).

However, the above mentioned requirement may not be sufficient to support the link between neuronal activity and behavioral choices. Especially when considering that the variability in neuronal responses to identical stimuli can have different origins, some of which may not be related to the behavioral outcome at all (Haefner et al. 2013). So, how can we disentangle the influence that neurons in sensory areas have on decisions, if any?

Historically, there are two main approaches trying to explain the problem regarding the relationship between sensory neuronal activity and decision outcomes. The first is known as the bottom-up interpretation, it is the most straightforward and supports a causal approach, in which variability in choices emerges from random fluctuations in the response of sensory neurons to external stimuli (Shadlen et al. 1996). The second is the top-down interpretation, it is non-causal and states that variability in choices reflects fluctuations in the influence of cognitive factors (e.g., attentional signals or intrinsic biases) on sensory neurons (Nienborg and Cumming 2009).

In order to determine which of these two approaches are involved in different decision making processes, there is a need for a unified generalizable model (Nienborg, R. Cohen, and Cumming 2012; Najafi and Churchland 2018). Such a model must include bottom-up and top-down origins of variability in sensory neuronal responses, and study their contributions to upcoming decisions in controlled conditions.

In the present work I will study a particular model of decision making and argue that an extension of its sensory neurons enables a direct way to differentiate bottom-up and top-down contributions to upcoming decision. The claim relies in the proposition that sensory neurons transmit different information streams through different spiking patterns. Thus, suggesting a biologically plausible, simple and generalizable method to tackle the interpretation problem regarding decision making.

1.1 Perceptual decision making

Perceptual decision making aims to relate the activity of sensory neurons to behavioral choices during controlled experimental tasks. In a perceptual task, subjects attend to a given sensory stimulus and report their understanding or *percept* of the external evidence as a decision. If information regarding the sensory integration of external evidence is added, the neuronal mechanisms contributing to the decision making process can be identified (Resulaj et al. 2009). Thus, by combining psychophysical and physiological techniques, the formation of decisions during simple perceptual tasks can be studied (Gold and Shadlen 2007).

A perceptual task involves a selection between choices based on sensory evidence, while the subject's performance is assessed. In general, the choices represent the detection of specific external stimuli. For example, imagine that a pattern of random dots is presented in front of you, and you must evaluate their net direction of motion. A choice will be associated with perceiving a majority of dots moving towards a specific direction.

In a two-choice simplification of the latter task, the net movement of dots is constrained to two options (e.g., *left* and *right*). If all dots move coherently towards one side, the task will be easy and your performance will be high for most cases. On the other hand, when all dots move randomly (i.e., there is no coherence between them), the expected choice is unknown and your performance will be at chance level.

In the latter scenario, you will select *left* for half of the cases and *right* for the other half. For each case, you are reporting your choice as an unbiased decision, because the sensory evidence is similar for both alternatives. This means that zero-coherent stimuli trigger similar neuronal activity, which in turn yields different choices. If fluctuations in the activity of sensory neurons to different presentations of identical stimuli predict the behavioral choice, then sensory neurons may encode information related to upcoming decisions (Parker and Newsome 1998).

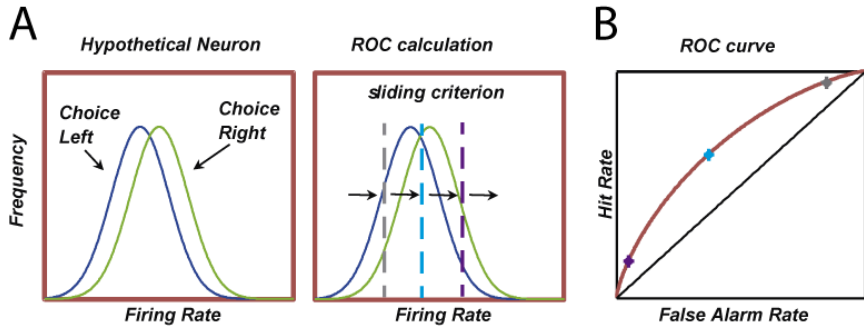


FIGURE 1.1: Measuring and calculating choice probability. (A) Two distributions of firing rates for a hypothetical neuron measured during the RDM task. Each distribution represents a choice (e.g., *left* or *right*) and their difference is quantified through the ROC analysis. (B) The ROC curve is obtained by sliding a threshold across the two distributions and integrating the area that exceeds each threshold. Three example thresholds are shown. The area under the ROC corresponds to CP. All panels adapted from Crapse and Basso (2015).

In the field of perceptual decision making, the above mentioned task is known as Random Dot Motion (RDM) task and it is often used to study decisions under controlled conditions (Gold and Shadlen 2007; Nienborg, R. Cohen, and Cumming 2012). More importantly, it is possible to have simultaneous physiological recordings of key sensory areas when using animal models. Thus, a link between sensory neuronal activity and behavior arises, gauging the relationship between the neural correlates encoding external stimuli and behavioral choices.

1.1.1 Sensory neuronal activity correlates with choices

Choice probability (CP) is a measure of the correlation between fluctuations in sensory neuronal activity and behavioral choices (Britten et al. 1996). The CP metric is an approach derived from signal detection theory, and quantifies how well a behavioral choice can be predicted from single neuronal activity (Crapsse and Basso 2015). Briefly, the firing rate of a neuron is recorded during a perceptual task (e.g., the two-choice RDM task). A receiver operating characteristic (ROC) curve can be constructed by identifying the two firing rate distributions according to each decision outcome (Figure 1.1A). CP is the area under the ROC curve (Figure 1.1B), and represents the probability that the neuron exhibits higher firing rate when the decision outcome is paired with its preferred stimulus (Nienborg, R. Cohen, and Cumming 2012).

In various sensory areas, there are consistent reports of CP significantly predicting upcoming decisions (Gold and Shadlen 2007). A relevant region when studying perceptual decision making through the RDM task is the sensory cortical area MT/V5. Neurons in MT are known to process motion sensitivity to visual stimuli, and can predict the decision-maker's choice with average values ~ 0.55 during the RDM task (Britten et al. 1996). At first sight, a 0.55 value of CP may indicate a weak relationship between sensory neuronal activity and behavioral choices. However,

MT neurons integrate external evidence and relay information to other associative areas, in which decisions are formed. Therefore, it results meaningful that information related to upcoming choices is embedded in the firing rate of single sensory neurons, located at early stages of the decision making process (Nienborg, R. Cohen, and Cumming 2012).

Additionally, neurons in MT preferably respond to stimuli with a particular direction of motion, and exhibit higher responses according to the strength of the motion signal (Britten et al. 1996). External stimuli are known to be encoded at a population level; so that a particular direction of motion is represented by a group of ~100 sensory neurons (Nienborg, R. Cohen, and Cumming 2012). This means that during the RDM task, there must then exist a population of MT neurons tuned to dots moving *left* and another to dots moving *right*. Furthermore, the activity of each population will increase according to the strength of their preferred direction of motion. In terms of coherence, the higher the coherence between moving dots, the higher the population response will be. The way MT neurons encode visual stimuli leads to competition between populations preferring opposite directions of motion (Cumming and Nienborg 2016). This means that every behavioral choice will be correlated with the activity of a particular population.

1.1.2 Sensory neural fluctuations emerge from different origins

Before moving on, let us review the pieces acting in the proposed decision making process. First, correlated activity is necessary to obtain a relationship between sensory neuronal responses and upcoming decisions. Sensory neurons within the same population are known to exhibit positive noise correlations, given that they are tightly *wired together* and share common inputs (Nienborg, R. Cohen, and Cumming 2012). Whereas, sensory neurons across populations exhibit negative correlations, given that the populations behave in a competitive setup (Wimmer et al. 2015; Cumming and Nienborg 2016).

Second, sensory neurons encode external stimuli as populations, rather than as single units. This encoding highlights the reliability principle in the brain, but also hides the specific origin of neuronal variability (Shadlen et al. 1996; Nienborg, R. Cohen, and Cumming 2012). Neuronal activity is known to vary with respect to three possible origins: fluctuations in external stimuli, intrinsic noise or fluctuations in top-down signals (Nienborg and Cumming 2009; Wimmer et al. 2015). The population of neurons encoding a particular percept will be correlated with its associated decision outcomes. However, the origins of the correlated activity can not be easily disentangled. When studying the relationship of sensory neurons to upcoming decisions, it is then crucial to assess the origin of neuronal fluctuations.

At this point we have reached the interpretation problem regarding CP: if correlation does not necessarily imply causation, how can we interpret the relationship

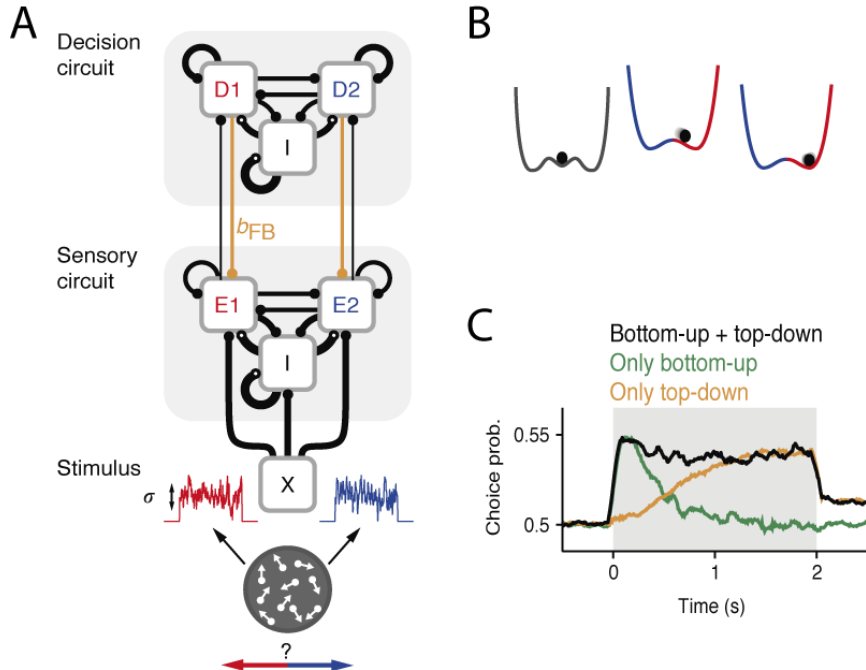


FIGURE 1.2: Hierarchical network model for decision making. (A) Network architecture: stimulus-selective populations E1 and E2 in the sensory circuit are coupled to choice-associated populations D1 and D2 in the decision circuit. There are feedforward and feedback (strength b_{FB}) connections between the two circuits, as well as inhibitory (I) and lateral excitatory recurrent connections. The width of lines represents connection probability and synaptic efficacy. (B) Commitment to a choice corresponds to a well in the energy-landscape of the decision process. (C) Sustained choice probability arises from the combination of early bottom-up and late top-down influences. All panels adapted from Wimmer et al. (2015).

between the activity of sensory neurons and upcoming decisions? The bottom-up interpretation states that the activity in sensory neurons is causally correlated with the upcoming decision, and that the correlations are established through random fluctuations in the response of sensory neurons to external stimuli. The top-down interpretation states that sensory activity reflects the building of choices in decision-related regions, and that correlated activity in sensory neurons is a response to fluctuations in feedback signals from upstream cortical regions. So, how can this ambiguity be solved?

1.2 Hierarchical network for perceptual decision making

An answer to the interpretation problem of choice probability appeared when Wimmer et al. (2015) proposed a hierarchical network model for perceptual decision making. In it, a sensory region receives bottom-up and top-down connections that can be systematically isolated from one another.

The network models a two-choice RDM task and accounts for the interactions between external stimuli, a sensory circuit and a decision circuit (Figure 1.2A). Stimulus-selective populations in the sensory circuit (E_1 and E_2) integrate fluctuations in external stimuli, and feedforward sensory evidence to analogous stimulus-selective populations in the decision circuit (D_1 and D_2). Moreover, the decision populations feedback the choice-related activity to the respective populations in the sensory circuit (orange connections, strength b_{FB}).

Specifically, the decision circuit is the canonical model for decision making proposed by Wang (2002). It is defined as a *winner-take-all* attractor network, in which each choice is a stable state equivalent to a well in the energy landscape of the decision process (Figure 1.2B). The network is at a resting stable state in the absence of external fluctuations. As soon as an external stimulus is presented, the attractor dynamics of the network will trigger a commitment to one of the two choices. In general, a stable state can be maintained unless a strong external stimulus is added to the network (Urai and Murphy 2016).

Using the network's setup and hierarchy, Wimmer et al. (2015) studied the different contributions of sensory neurons to upcoming decisions in different connectivity conditions. In the bottom-up condition, the sensory circuit receives different presentations of zero-coherence external stimuli, and has no feedback from the decision circuit. When CP was calculated, a decaying trace appeared simultaneously with stimulus onset (Figure 1.2C, green trace). This result is consistent with experimental data from macaque monkeys performing a two-choice RDM task (Nienborg and Cumming 2009). Overall, these results indicate that bottom-up fluctuations in sensory neurons exert a causal influence on upcoming decisions at early stages of the decision making process.

In the top-down condition, the sensory circuit receives multiple presentations of identical zero-coherence stimuli, and has weak feedback from the decision circuit. This set up decreases neuronal variability after stimulus onset given the repeated presentations of identical stimuli (Churchland et al. 2010). Moreover, because the external stimulus is always the same, the remaining variability in sensory responses is known to be influenced only by top-down signals (i.e., there are no bottom-up fluctuations). When CP was calculated, a slowly increasing trace appeared, which ramped up following the activity in the decision circuit (Figure 1.2C, orange trace). As the decision circuit integrates evidence and *selects* a choice, it influences sensory activity through feedback connections. Overall, these results indicate that top-down correlations influence upcoming decisions at late stages of the decision making process.

If analyzed by themselves, neither the bottom-up nor top-down components of CP explain the sustained, plateau-like traces observed in sensory neurons during experimental conditions (Britten et al. 1996). However, when adding both components, a sustained CP trace appears throughout the stimulus presentation (Figure 1.2C, black trace). Thus, Wimmer et al. (2015) results identify the underlying

mechanisms of neuronal variability during perceptual decisions, and solve the ambiguous interpretation of CP. Their elegant analysis suggests that sensory neurons correlate with upcoming decisions following both the bottom-up and the top-down interpretation. Early in the decision making processes, bottom-up fluctuations in sensory activity exert a causal influence on the upcoming decision. On the other hand, top-down influences on upcoming decisions appear at late stages of the decision making processes.

1.2.1 Model limitations

As previously suggested in the field of perceptual decision making (Nienborg, R. Cohen, and Cumming 2012), both bottom-up and top-down interpretations are involved in linking neuronal activity with behavior. The findings by Wimmer et al. (2015) are an elegant proof supporting the involvement of both interpretations, and further investigate the time-course in which each influence appears during a two-choice RDM task.

In an *a posteriori* understanding, it is reasonable to think about the temporal identification of both mechanisms. Sensory circuits process external evidence immediately after stimuli are presented, according to diverse feature-tuning patterns. Then, the sensory evidence is fed to decision-related areas, which reach a choice after the evidence has accumulated. However, this distinction was obtained under specific conditions, in which neither the external stimuli nor intrinsic top-down signals bias the selection of a choice.

Therefore, the outstanding results of Wimmer et al. (2015) come at a loss of generalization. For sure, certain decision making processes are explained by sensory neural activity with an early, bottom-up and a late, top-down influence on choice. But, do all decision making networks behave this way? What about decision making processes in which sensory evidence is entirely disregarded? Or when decisions are merely influenced by intrinsic biases?

In order to compare the bottom-up and top-down influences on CP under different conditions, different models for each condition must be evaluated. The problem is that these models are complex and dependent on knowledge related to the neuronal circuits involved in each decision making task. So that, the development of different decision making networks requires exhaustive research and accurate abstraction according to each condition.

Furthermore, the systematic variation of bottom-up and top-down contributions to upcoming decisions can not be achieved during normal, physiological conditions. For example, it will be very difficult to eliminate bottom-up fluctuations in order to evaluate the isolated effect of top-down signals during an actual experiment. And it will be similarly difficult to study decision networks with various types of stimuli or different top-down signals. Thus, the hierarchical network model for perceptual

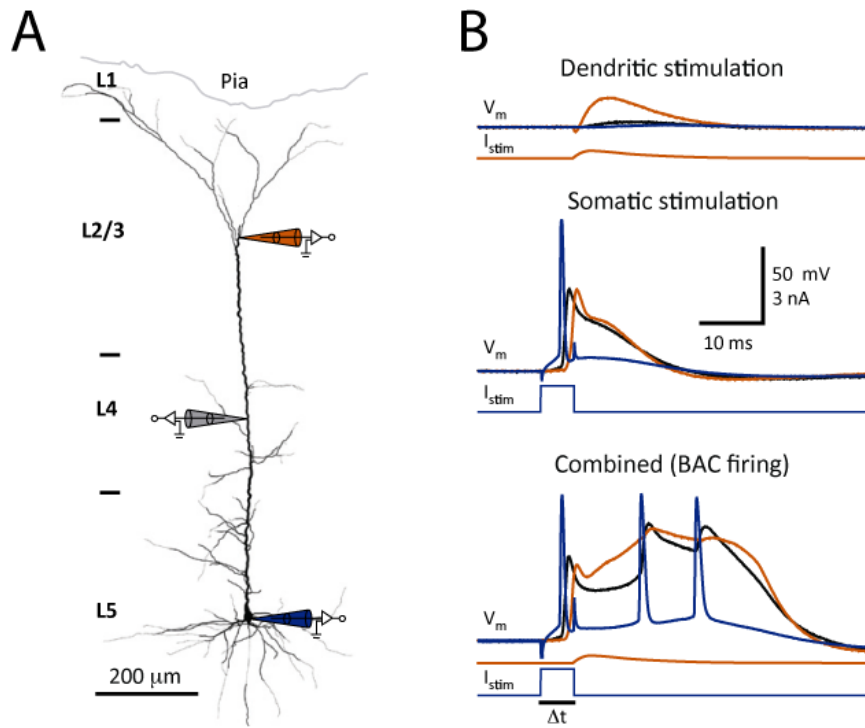


FIGURE 1.3: Anatomy and bursting mechanism of L5 pyramidal neurons. (A) Soma (blue) and distal dendrites (orange) of L5 pyramidal neurons extend through all the layers of sensory cortex. (B) The bursting mechanism in L5 pyramidal neurons is explained through a triple recording experiment. (Top) Distal excitatory input (I_{stim} , red) causes no dendritic spike (orange) and has virtually no impact at the soma (blue). (Middle) A somatic action potential evoked with somatic current injection (I_{stim} , blue) invades the dendritic tree but still causes no dendritic spike. (Bottom) Combined injection of the same dendritic and somatic inputs as in the upper panels reaches threshold for a dendritic calcium spike which triggers burst firing. All panels from Larkum (2013).

decision making proposed by Wimmer et al. (2015) results in an indirect and expensive method to disentangle bottom-up and top-down contributions to upcoming decisions when studying different decision making networks.

1.3 Extended hierarchical network

In this thesis, I propose a simple analysis to address some of the limitations of the hierarchical network and thus, gain generalization regarding the study of different decision making processes. The method relies both on the architecture of sensory cortical areas, and on important electrophysiological properties of excitatory neurons. As a proof of concept, I construct an extended version of the hierarchical network, in which the sensory excitatory neurons are modeled using more biological, two-compartment neurons.

1.3.1 Motivation

The sensory cortex exhibits a layered architecture, in which each layer is clearly distinguished by the main neuronal types found therein. Overall, excitatory neurons make up to 70-80% of the neural population (Larkum 2013), while the rest are various types of inhibitory interneurons. Interestingly, sensory external inputs (i.e., bottom-up signals) arrive at intermediate cortical layers, whereas feedback inputs from associative cortical areas (i.e., top-down signals) project to outer cortical layers (Larkum 2013).

Within this architecture, the layer 5 excitatory pyramidal neurons (from now on L5 pyramidal neuron) is relevant given its anatomy (Figure 1.3A). Its distal dendrites spread to the outermost layers, and receive top-down signals. On the other hand, its apical dendrites sit in the intermediate layers near the soma and receive bottom-up signals (Larkum 2013; D’Souza and Burkhalter 2017). Thus, L5 pyramidal neurons function as key computational units because of their capacity to detect two streams of information separately. Most importantly, they combine both streams when associations between sensory external evidence and internal representations must be formed (Larkum 2013).

Physiologically, the combination of both streams of information occurs via the neuron’s intrinsic bursting mechanism. Bursting in L5 pyramidal neurons emerges when single somatic spikes are back-propagated to the apical dendrite and temporally coincide with feedback inputs to the distal dendrites (Figure 1.3B). The combination of inputs is sufficient to trigger the dendritic Ca^{2+} engine of L5 pyramidal neurons. When the engine is activated, long-lasting, self-propagated Ca^{2+} spikes reach the axon initiation zone and trigger bursts, given the high-frequency firing (Larkum, Zhu, and Sakmann 1999). In the absence of combined inputs, the dendritic Ca^{2+} engine is seldom activated, and no associations between sensory evidence and internal representations are formed (Major, Larkum, and Schiller 2013).

Currently, a detailed understanding of how information is transmitted in the sensory cortex is missing. Most often, for the sake of simplicity, neural network models disregard both the cortical layered architecture and the paradigmatical functionality of L5 pyramidal neurons. However, recent literature (Manita et al. 2017; Stuart and Spruston 2015) emphasizes the importance of dendritic bursts in information processing and in the ability to execute cognitive functions (e.g. perception, decision making, memory). When dealing with theoretical models of cognitive functions, it is then important to consider the two remarkable characteristics of the sensory cortex. Hence, I propose to replace the sensory excitatory neurons in the hierarchical network by L5 pyramidal neurons, and assess the network’s representation of the bottom-up and the top-down information streams.

1.3.2 Two-compartment model for sensory pyramidal neurons

A mathematical model of the relevant properties of L5 pyramidal neurons was recently developed by Naud and Sprekeler (2018). The model divides the neurons in two compartments: dendrite and soma, which are constrained by electrophysiological recordings to capture intrinsic bursting. Communication between compartments is possible through the forward and back-propagation of dendritic Ca^{2+} activity. One motivation behind the two-compartment model is to represent the bottom-up and top-down information streams through distinguishable spiking patterns.

The capacity of simultaneously representing information from different sources with minimal cross-talk is known as multiplexing. In the case of L5 pyramidal neurons, the two different sources are the bottom-up and top-down information streams, and their information may be encoded through distinguishable spiking patterns. In the firing rate A of a neuron there are both single spikes and bursts. Bursting occurs when there is combined input to the soma and dendrites of L5 pyramidal neurons (Larkum, Zhu, and Sakmann 1999). Thus, the proportion of single spikes converted into bursts (i.e., burst fraction F) may represent the dendritic input, which in turn mainly comprises top-down signals. The somatic input mainly involves bottom-up signals, and thus, can be tracked by either the occurrence of a single spike or a burst (i.e., event rate E). Hence, a multiplexed neural code can be achieved by distinguishing events from bursts. A more detail description of the latter spiking analysis is given in Section 2.3.

Indeed, Naud and Sprekeler (2018) show that the two-compartment representation of L5 pyramidal neurons enables multiplexing at a population level. Bottom-up signals are encoded through the event rate E , whereas top-down signals are encoded in the burst fraction F of a population of L5 pyramidal neurons. Furthermore, their findings can easily be compared using different network models and validated using experimental data, because they are obtained through a simple spiking analysis.

In particular, the idea fits well within the context of the hierarchical network for perceptual decision making. The replacement of sensory neurons by two-compartment L5 pyramidal neurons could lead to different streams of information being encoded in distinguishable spiking patterns. And thus, to a direct method for disentangling the bottom-up and top-down contributions on CP. Hence, this thesis investigates the idea of multiplexing in an extended hierarchical network model for perceptual decision making with two-compartment pyramidal neurons. Moreover, it aims to relate the information encoded in the different spiking patterns of sensory pyramidal neurons with the bottom-up and the top-down information streams involved in a perceptual decision making process.

Chapter 2

Methods

In the following chapter, I will explain the details behind the models and analysis used in this thesis. I will also elaborate on the selection of important parameters for each model, with an emphasis on the implementation of the two-compartment model for sensory neurons within the hierarchical network. For an exhaustive description of model parameters, refer to Supplementary Tables 1-4 in Wimmer et al. (2015), and Table S1 in Naud and Sprikeler (2018). Unless otherwise stated, the same parameter values as the original models are used.

2.1 Hierarchical network

The network model for perceptual decision making proposed by Wimmer et al. (2015) consists of a sensory circuit connected to a decision circuit, which responds to a two-choice RDM task (see Figure 1.2). The sensory circuit aims to model the activity seen in cortical area MT/V5, which contains direction-selective neurons (E1 and E2). The decision circuit models the decision-related activity observed in LIP/FEF, which contains neurons that act as evidence accumulators until a decision threshold is reached (D1 and D2). This decision circuit is a well-known neurobiological principled model of decision making (Wang 2002). There are feedforward connections from sensory to decision circuits, and feedback from decision to sensory (orange connections). This feedback connections represent the top-down stream of information to sensory neurons during perpetual decision making. On the other hand, the bottom-up stream of information is represented by external sensory information arriving to the sensory circuit as time-varying Ornstein-Uhlenbeck input currents.

The sensory and decision circuits contain two stimulus-selective populations, each representing one of the two directions of motion. Neurons within the same populations share strong recurrent synapses (with potentiating factor $w_+=1.3$ and 1.6, for sensory and decision circuits, respectively). In contrast, neurons across populations respond to opposite directions of motion (i.e., *they fire out of sync*), which leads to a weaker coupling between them ($w_-=0.7$ and 0.9, for sensory and decision circuits, respectively).

	E	$E^{(s, d)}$	I		E	I		
$\bar{g}_{E,\text{AMPA}}$	0.76	1.0508	1.52	nS	$\bar{g}_{E,\text{AMPA}}$	0.05	0.04	nS
$\bar{g}_{I,\text{GABA}_A}$	12.6	17.5156	12.6	nS	$\bar{g}_{E,\text{NMDA}}$	0.165	0.13	nS
$\bar{g}_{X,\text{AMPA}}$	1.71	2.3645	1.71	nS	$\bar{g}_{I,\text{GABA}_A}$	1.3	1.0	nS
$\bar{g}_{FB,\text{AMPA}}$	0.0668	0.0971	-	nS	$\bar{g}_{X,\text{AMPA}}$	2.1	1.66	nS
(A) Sensory circuit				(B) Decision circuit				
					$\bar{g}_{FF,\text{AMPA}}$	0.0668	-	nS

TABLE 2.1: Mean efficacies of synaptic conductances in hierarchical network. Conductances with a post-synaptic target in the sensory (A) and in the decision circuit (B). E indicates excitatory neurons, $E^{(s, d)}$ refers to L5 pyramidal neurons, I inhibitory neurons, X external population, FB feedback connections from the decision circuit and FF feedforward connections from the sensory circuit.

2.1.1 Sensory circuit

The sensory circuit is formed by 1600 excitatory (E) and 400 inhibitory neurons (I); the two-stimulus selective excitatory populations (i.e., E1 and E2) include 800 neurons each. The membrane potential u of each neuron k is modeled as leaky integrate-and-fire units as follows:

$$\frac{d}{dt}u_k = -\frac{(u_k - E_L)}{\tau_m} + \frac{I_{\text{stim},k} + I_{\text{syn},k}}{C_m} \quad (2.1)$$

where $E_L = -70$ mV is the reversal potential, $\tau_m = 15$ ms the timescale of the membrane potential, $C_m = 250$ pF the membrane capacitance, $I_{\text{stim},k}$ the external stimulus and $I_{\text{syn},k}$ encompasses the synaptic contributions from recurrent and external connections. Overall, the synaptic contribution I_{syn} is described by:

$$I_{\text{syn}} = I_{E,\text{AMPA}} + I_{I,\text{GABA}_A} + I_{X,\text{AMPA}} + I_{FB,\text{AMPA}} \quad (2.2)$$

because neurons in the sensory circuit receive excitatory and inhibitory recurrent contributions with a probability $p=0.2$ ($I_{E,\text{AMPA}}$ and I_{I,GABA_A} , respectively). In addition, sensory neurons receive excitatory background activity from 1000 external neurons (X) firing Poisson spike trains at a rate $\nu_{\text{ext}}=12.5$ sp s $^{-1}$ ($p_x=0.32$, $I_{X,\text{AMPA}}$). Moreover, populations E1 and E2 receive feedback excitatory inputs $I_{FB,\text{AMPA}}$ from respective populations in the decision circuit ($p_{FB}=0.2$, see Figure 1.2A for a diagram of the circuit). Excitatory synapses mimic AMPA conductances, whereas inhibitory synapses mimic GABA_A conductances. The synaptic reversal potentials for excitatory and inhibitory synapses are $E_E=0$ mV and $E_I=-80$ mV, respectively. The mean efficacies of synaptic conductances in the sensory circuit are shown in Table 2.1A.

The replacement of sensory excitatory neurons by two-compartment L5 pyramidal neurons is done as follows. A L5 pyramidal neuron is modelled as a somatic and a dendritic region communicating with one another through the dendritic Ca²⁺ engine (Naud and Sprekeler 2018).

The somatic compartment follows leaky integrate-and-fire dynamics with spike-triggered adaptation, which is included through the time-varying recovery variable $w^{(s)}$ (Equation 2.4). Thus, the somatic membrane potential $u^{(s)}$ of neuron k is described by:

$$\frac{d}{dt}u_k^{(s)} = -\frac{u_k^{(s)} - E_L}{\tau_m^{(s)}} + \frac{g_s f(u_k^{(d)}) + I_{k,s}^{(s)} + w_i^{(s)}}{C_m^{(s)}} \quad (2.3)$$

$$\frac{d}{dt}w_k^{(s)} = -\frac{w_k^{(s)}}{\tau_w^{(s)}} + b_w^{(s)} S_k^{(s)} \quad (2.4)$$

where the reversal potential $E_L = -70$ mV, the membrane time constant $\tau_m^{(s)} = 16$ ms and the membrane capacitance $C_m^{(s)} = 370$ pF. $g_s = 1300$ pA controls the forward propagation of dendritic Ca^{2+} activity. $I_{\text{stim},k}^{(s)}$ is the external stimulus. $\tau_w = 100$ ms and $b_w = -200$ pA are the timescale and strength of spike-triggered adaptation $w^{(s)}$, and $S_k^{(s)}$ corresponds to the spike train of neuron k .

The dendritic compartment accounts for Ca^{2+} dynamics using the sigmoidal non-linear function f , and further includes sub-threshold adaptation through the time-varying recovery variable $w^{(d)}$. The following describe the dendritic membrane potential $u^{(d)}$ of neuron k :

$$\frac{d}{dt}u_k^{(d)} = -\frac{u_k^{(d)} - E_L}{\tau_m^{(d)}} + \frac{g_d f(u_k^{(d)}) + c_d K(t - \hat{t}_k^{(s)}) + w_k^{(d)}}{C_m^{(d)}} \quad (2.5)$$

$$\frac{d}{dt}w_k^{(d)} = -\frac{w_k^{(d)} + a_w^{(d)}(u_k^{(d)} - E_L)}{\tau_w^{(d)}} \quad (2.6)$$

where the reversal potential $E_L = -70$ mV, the membrane time constant $\tau_m^{(d)} = 7$ ms and the membrane capacitance $C_m^{(d)} = 170$ pF the membrane capacitance. $g_d = 1200$ pA controls the local Ca^{2+} regenerative activity described by $f(\cdot)$. The back-propagation of somatic spikes $\hat{t}_k^{(s)}$ is modeled through K and scaled by $c_d = 2600$ pA. $\tau_w = 30$ ms and $a_w = -13$ pA are the timescale and strength of sub-threshold adaptation $w^{(d)}$.

Somatic units receive the external stimulus $I_{\text{stim},k}$, lateral $I_{\text{E,AMPA}}$ and inhibitory $I_{\text{I,GABA}_A}$ recurrent contributions, and background excitatory activity $I_{\text{X,AMPA}}$ from the external Poisson population X. Dendritic units receive top-down excitatory inputs $I_{\text{FB,AMPA}}$ from the decision circuit and background inhibitory activity $I_{\text{OU,GABA}_A}$ from a time-dependent Ornstein-Uhlenbeck process (with $\mu = -270$ pA, $\sigma = 450$ pA and $\tau = 2$ ms) independently drawn for each unit. Thus, somatic and dendritic synaptic contributions are:

$$I_{\text{syn}}^{(s)} = I_{\text{E,AMPA}} + I_{\text{I,GABA}_A} + I_{\text{X,AMPA}} + I_{\text{FB,AMPA}} \quad (2.7)$$

$$I_{\text{syn}}^{(d)} = I_{\text{FB,AMPA}} + I_{\text{OU,GABA}_A} \quad (2.8)$$

The mean synaptic efficacies are scaled with respect to the leak conductance $g_L = \frac{C_m}{\tau_m}$ for each compartment (Table 2.1), in order for the sensory circuit to maintain an

analogous behavior to that in the original hierarchical network.

2.1.2 Decision circuit

The decision circuit acts as an attractor network, in which each decision corresponds to an attraction state in an energy landscape (see Figure 1.2). It contains 1600 excitatory (E) and 400 inhibitory (I) leaky integrate-and-fire neurons. The excitatory neurons are divided into three populations: the stimulus-selective populations D1 and D2 (240 neurons each) and the non-specific population Dn (i.e., the rest). This division is a simple generalization of experimental conditions, in which there are fewer neurons selective for the external stimuli in associative areas.

The membrane potential u of each neuron k is defined by:

$$\frac{d}{dt}u_k = -\frac{(u_k - E_L)}{\tau_m} + \frac{I_{\text{syn},k}}{C_m} \quad (2.9)$$

with $E_L=-70$ mV, $\tau_m^E=20$ ms and $\tau_m^I=12.5$ for excitatory and inhibitory neurons, respectively. Again, I_{syn} encompasses the synaptic contributions from recurrent and external connections, such that:

$$I_{\text{syn}} = I_{E,\text{AMPA}} + I_{E,\text{NMDA}} + I_{I,\text{GABA}_A} + I_{X,\text{AMPA}} + I_{FF,\text{AMPA}} \quad (2.10)$$

because the synaptic dynamics mimic AMPA, GABA_A and non-linear excitatory NMDA conductances. All neurons in the decision circuit receive full excitatory and inhibitory recurrent connections ($p=1$) and excitatory background activity through AMPA synapses from independent Poisson spike trains ($p_x=1$, $\nu_{\text{ext}}=2392$ sp s⁻¹ for D1 and D2, $\nu_{\text{ext}}=2400$ sp s⁻¹ for Dn and I). Moreover, each neuron in populations D1 and D2 receives feedforward AMPA synapses from respective populations in the sensory circuit ($p_{FF}=0.2$, see Figure 1.2A for a diagram of the circuit). The synaptic reversal potentials for excitatory and inhibitory synapses are $E_E=0$ mV and $E_I=-70$ mV, respectively. The mean efficacies of the synaptic conductances involved in the decision circuit are shown in Table 2.1B.

Populations D1 and D2 act as evidence accumulators due to the long-lasting recurrent activity enabled by NMDA conductances ($\tau_{\text{NMDA}}=100$ ms, as opposed to $\tau_{\text{AMPA}}=2$ ms or $\tau_{\text{GABA}_A}=5$ ms). This network is considered a *canonical* spiking model for decision making (Wang 2002; Nienborg, R. Cohen, and Cumming 2012; Gerstner et al. 2014) and has been extensively studied.

2.1.3 External stimulus

In order to represent a RDM task, the movement of dots is converted to random input currents which drive the sensory circuit. There are two possible directions of movement (e.g., *left* and *right*), each one modeled as independent, time-evolving Ornstein-Uhlenbeck processes. Each process forms an afferent current to different populations of sensory excitatory neurons (from now on E1 and E2), maintaining

the direction selectivity observed in these neurons. Thus, a stimulus input current to neuron k is defined as:

$$I_{\text{stim},k}^{\beta}(t) = I_0(s^{\beta}(t) + s_k^{\beta}(t)), \quad (2.11)$$

with $I_0=80$ pA, the mean input current for zero-coherence stimuli. The terms $s^{\beta}(t)$ and $s_k^{\beta}(t)$ correspond to common and private stimulus realizations to population β , with $\beta=(\text{E1}, \text{E2})$. This represents the common input within neurons of the same population, while also enabling heterogeneity across individual sensory neurons. Thus, the first term is common to all neurons in population β and independent across populations. Whereas, the second term is independent to each neuron k , regardless if k belongs to population β . Both terms are given by:

$$s^{\beta}(t) = 1 + c\gamma^{\beta} + \sigma_{\text{stim}}z^{\beta}(t) \quad (2.12)$$

$$s_k^{\beta}(t) = \sigma_{\text{ind},k}z_k^{\beta}(t), \quad (2.13)$$

where c is the stimulus coherence and γ^{β} represents the mean input at highest coherence ($\gamma^{\beta}=0.25$ and -0.25 for $\beta=\text{E1}$ and E2 , respectively). $z^{\beta}(t)$ and $z_k^{\beta}(t)$ are independent Ornstein-Uhlenbeck processes with zero-mean, unit-variance and time constant $\tau_{\text{stim}}=20$ ms. The amplitude of the current inputs is controlled by the variables $\sigma_{\text{stim}}=\sigma_{\text{ind}}=0.212$.

2.2 Spike count statistics and choice probability

For each neuron k during a simulation run l , spike trains are converted into instantaneous spike counts $n_k^l(t; T)$ using a discrete convolution with a rectangular kernel of a specific count window ($T=50$ ms, unless otherwise specified). The average across simulation runs l of neuron k yields the individual trial-average rate $r_k(t) = \frac{1}{T}\langle n_k^l(t; T) \rangle_l$, whereas the average across neurons of the same population β during simulation run l yields the population rate $r_{\beta}^l(t) = \frac{1}{TN_{\beta}} \sum_k n_k^l(t; T)$. Since populations are symmetric, they exhibit interchangeable dynamics regardless which choice α was taken (with $\alpha=1,2$). Thus, populations are identified as *preferred* or *opposite* according to the outcome of the behavioral choice in each simulation run (i.e., *preferred* if the choice $\alpha = \beta$, and *opposite* if the choice $\alpha \neq \beta$).

Instantaneous choice probabilities $CP_k(t, T)$ are calculated for each neuron k by classifying the spike counts according to the *preferred* or *opposite* outcome in each simulation run l . The classification leads to two distinguishable distributions: $\{n_k^l(t; T)\}_{l \in \text{Preferred}}$ versus $\{n_k^l(t; T)\}_{l \in \text{Opposite}}$. The two distributions of spike counts are then evaluated at each time point t through a receiver operating characteristic analysis (ROC). Following this signal detection theory analysis, the area under the ROC represents the probability of neuron k exhibiting higher firing rate at time t , when being part of the *preferred* population, in comparison to when in the *opposite* population (Crapse and Basso 2015). Thus, CP values near 0.5 indicate chance performance, or that this

particular neuron is not related with the behavioral choice. For the instantaneous trace of CP, the count window $T=100$ ms, unless otherwise specified.

Spike count noise correlations are computed between neurons k and k' at times t and t' , via the Pearson correlation coefficient:

$$\rho_{k,k'}(t, t') = \frac{\text{Cov}[n_k^l(t; T), n_{k'}^l(t; T)]}{\sqrt{\text{Var}[n_k^l(t; T)]\text{Var}[n_{k'}^l(t; T)]}} \quad (2.14)$$

covariance and variance are obtained across simulation runs. Count window $T=250$ ms, unless otherwise specified.

Average CP and correlations were calculated for 100 randomly selected active neurons from populations E1 and E2 (i.e., 50 per population) over multiple simulations runs. Active neurons have a minimal firing rate of 1 sp s⁻¹ on each simulation run. Coefficient of variation C_V was obtained for each active neuron and averaged across simulation runs.

An additional measurement of the impact of stimulus fluctuations to behavioral choices was calculated using the *reverse correlation* method (Gerstner et al. 2014). This method defines the psychophysical kernel for sensory excitatory neurons as the average population stimulus leading to a particular choice (similar to the calculation of the spike-triggered averaged stimulus). Overall, this analysis closely follows the measurements described in Wimmer et al. (2015).

2.3 Burst coding and multiplexing

To disclose the two streams of information from each neurons' spiking patterns, Naud and Sprekeler (2018) propose a distinction between single spikes and bursts. A burst is defined as a minimum of two consecutive spikes with an inter-spike-interval (ISI) less than 16 ms, otherwise, the spikes represent singlets. An event is defined as a spiking pattern which is either a burst or a single spike. The length of a burst may vary, but short, sparse bursts (i.e., the less spikes included in one event) maximize information transmission.

Now, for each neuron k during a simulation run l , spike trains, burst trains and event trains are converted to instantaneous spike ($n_k^l(t : T)$), burst ($b_k^l(t : T)$) and event counts ($e_k^l(t : T)$) using again discrete convolutions with a rectangular kernel ($T=50$ ms, unless specified otherwise). The average across simulation runs of neuron k yields the individual trial-averaged firing rate ($r_k(t)=A_k(t)$), burst rate ($B_k(t)$) and event rate ($E_k(t)$). When averages are taken across neurons of the same population β during a simulation run l , the result are the population rates $r_\beta^l(t)=A_\beta^l(t)$, $B_\beta^l(t)$ and $E_\beta^l(t)$, respectively. Notice that the firing rate (A) will be equivalent to the event rate (E) only in the absence of bursts.

The theoretical analysis developed by Naud and Sprekeler (2018), shows that the event rate represents the bottom-up stream of information, because both single-spikes and bursts track the input arriving to the soma. On the other hand, the top-down stream of information is represented by the burst probability $F = B/E$, which is defined as the probability of converting a somatic spike into a burst. Recall that bursting is only possible via the conjunctive bursting mechanism of L5 pyramidal neurons (Larkum 2013, see chapter 1). Thus, the burst rate B encompasses both top-down inputs to the dendrites and the bottom-up inputs to the soma. Hence, top-down inputs to distal dendrites (i.e., F) can be isolated simply by normalizing the burst rate (B) with respect to the bottom-up contribution (E). For this work, I use the name neurometric analysis when referencing the calculation of A , B , E and F .

Instantaneous $CP_k(t, T)$ can be further calculated for each neuron k using event counts $e_k^l(t : T)$ or burst fraction counts (i.e., $\frac{b_k^l(t:T)}{e_k^l(t:T)}$). The respective outputs represent the CP calculated from the bottom-up (CP_E) and top-down (CP_F) signals encoded in E and F . In this thesis, I further compared the early and late components of CP with the proposed CP from E and F .

2.4 Simulation details

Based on code by Wimmer et al. (2015), the hierarchical network model was replicated in *Python* (version 3.6) using the spiking neural network simulator *Brian2* (versions 2.2). The code is available at: github.com/psrmx/decision_making. The Euler integration method was used for solving differential equations, with a time step of 0.1 ms.

For this work, the simulations included fixed-duration trials with a stimulus duration of 2 s, preceded and followed by a no-stimulus period between 0.5-1 s. On each trial, a behavioral choice is selected according to the decision population with the averaged highest rate in the final 0.5 s interval before stimulus offset. Psychometric curves for each network were computed varying the coherence parameter c from -1 to 1, and assessing the network's choice over 100 simulation runs. For convenience, $c=1$ corresponds to the choice $\alpha=1$.

Following Wimmer et al. (2015) analysis, results are based on 2,000 simulations runs for the *only bottom-up* and *fully connected* cases (as in Wimmer et al. (2015)), and over 1,000 simulations runs for the *only top-down* case (versus 10,000 in Wimmer et al. (2015)).

Moreover, the hierarchical network was set to be exactly the same to guarantee comparable results across different trials (Wimmer et al. 2015). This is achieved by using a specific random number generator seed when creating all the synaptic connections. In each trial, different stimuli realizations and different initial conditions were used, in order to model different experimental conditions.

Chapter 3

Results

The following chapter describes the main observations of the present thesis. The first task was to replicate the results on the hierarchical network by Wimmer et al. (2015), in order to obtain a functional model for perceptual decision making. Then, an extension of the hierarchical network using two-compartment sensory neurons was studied. The objective is to separate the two streams of information using a neural code able to distinguish single spikes from bursts, which is a characteristic of L5 pyramidal neurons (Naud and Sprekeler 2018). Finally, I assess to what extend bottom-up and top-down influences on CP can be directly decoded using the proposed multiplexed neural code.

3.1 Replication of hierarchical network

A single simulated trial of the replicated hierarchical network is shown in Figure 3.1A. The population-averaged stimuli (bottom panel) are fed to sensory populations E1 and E2 (middle panels) as input currents with mean $I_0=80$ pA. In turn, populations E1 and E2 send feedforward inputs to decision populations D1 and D2 (top panels). Moreover, decision populations D1 and D2 return feedback inputs to sensory populations E1 and E2 when top-down connections are present. The feedback parameter b_{FB} controls the presence and strength of the aforementioned top-down connections: $b_{FB}=0$ indicates no top-down connections, and $0 < b_{FB} < 6$ indicates the strength of top-down inputs by amplifying the mean efficacy (see Chapter 2). In Figure 3.1, b_{FB} is set to 0.

Raster plots of the sensory circuit (Figure 3.1A, middle panels) show how populations E1 and E2 in the sensory circuit respond to stimulus fluctuations. When comparing the population-averaged stimuli and the population-averaged responses of E1 and E2, a short lag of less than 5 ms is noticeable. The dominant population changes every ~ 150 ms due to the circuit's competitive regime, which is mediated by common inhibition (Wimmer et al. 2015; Machens, Romo, and Brody 2005). The sensory circuit operates in a balanced regime, and inhibitory activity (gray trace) is higher than excitatory activity (red and blue traces). Strong stimuli (>100 pA) trigger high population-averaged rates (>10 sp s $^{-1}$) in the sensory excitatory populations.

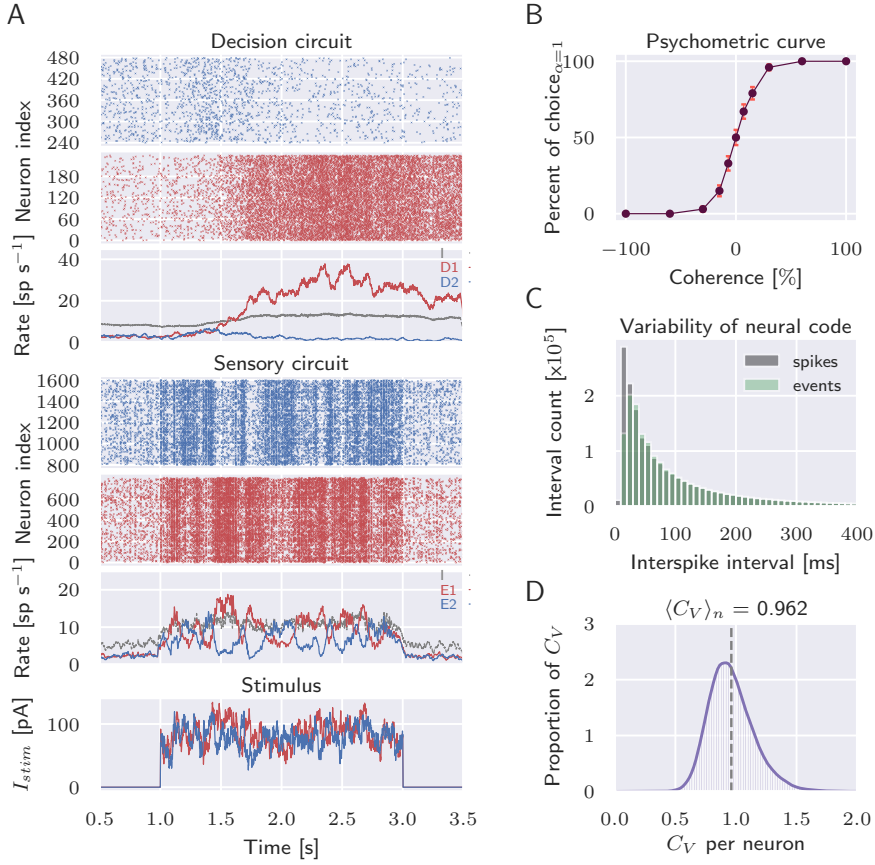


FIGURE 3.1: Hierarchical network models a RDM task. (A) Single response of the network to a zero-coherence external stimulus ($c=0$). Panels show population averages in the external stimulus (bottom), sensory (middle) and decision (top) circuits, and the rastergrams of the excitatory neurons from both circuits. (B) The psychometric curve shows the percentage of *preferred* $\alpha=1$ choices versus stimulus coherence (data plotted as mean \pm SEM). Spiking characteristics of sensory excitatory neurons are shown in the distributions of inter-spike intervals (C) and coefficient of variation C_V (D).

In these cases, the rate of the *opposite* population is suppressed to values as low as the activity elicited by the external background (2 sp s^{-1} , blue troughs).

The decision circuit (Figure 3.1A, top panels) responds to sensory evidence with slower dynamics than those observed in the sensory circuit, given the reverberations elicited by long-lasting NMDA conductances (Wang 2002). Raster plots show the strong, *winner-take-all* competition between stimulus-selective populations D1 and D2. Furthermore, high population rates in the sensory circuit, which appear when strong stimuli are present, trigger the formation of behavioral choices in the decision circuit. This is clear when noticing the jump in activity ~ 0.5 seconds after stimulus onset.

The stimulus represents the random movement of dots during a RDM perceptual task (Figure 3.1A, bottom panels). The coherence parameter c signals the proportion

of dots moving towards the same direction: $c > 0$ indicates movement towards the direction *preferred* by population E1, $c < 0$ towards the direction *preferred* by population E2, and $c = 0$ is an unbiased stimulus. In Figure 3.1B, the behavioral response of the hierarchical network to varying c is shown. The trace follows the classical sigmoidal shape observed in various psychophysics experiments and more importantly, it follows the recorded activity from MT neurons during a RDM task (Shadlen et al. 1996). Moreover, the hierarchical network is unbiased towards a preferred direction of motion; that is, when stimuli have zero-coherence the network performs at chance level. However, the unbiased behavior was highly dependent on the seed used to generate the network's connections (data not shown, similar observations were reported by Wimmer et al. (2015)).

An in-depth description of the spiking patterns observed in sensory excitatory neurons is presented in Figure 3.1C, D. The inter-spike interval (ISI) distribution (Figure 3.1C) indicates that spiking in sensory neurons follows a Poisson process, with an average interval between 10-20 ms (absolute refractory period $\tau_{\text{ref}}^E = 2$ ms). Moreover, the comparison with the ISI distribution from an event-based neural code (green distribution) reveals a low presence of bursts. A burst is considered to have a maximal ISI between consecutive spikes of 16 ms (Naud and Sprekeler 2018), and the average burst size is 2.2 sp per burst (data not shown). Thus, spikes in the smallest bin (0-10 ms) indicate the relative occurrence of bursts in sensory excitatory neurons (average burst fraction $F \sim 5\text{-}6\%$, data not shown). Sensory excitatory neurons present a mean $C_V = 0.962$ (Figure 3.1D), which further supports Poisson-like spiking with an absolute refractory period (i.e., C_V slightly below 1).

The present implementation of the hierarchical network successfully reproduces the results regarding the bottom-up and top-down influences on CP (Figure 3.2). Systemically changing the network's architecture through the feedback amplification variable b_{FB} enables the study of the network with only bottom-up correlations (Figure 3.2A-C), and only top-down connections (Figure 3.2D-F) by additionally presenting a set of replicated stimuli.

Population-averaged firing rates for the decision and sensory circuits are shown in Figure 3.2A, D. The behavior of the decision circuit is similar with and without top-down connections: the *preferred* population slowly increases its firing rate, which in turn causes stronger inhibition of the *opposite* population due to the *winner-take-all* dynamics. There is a slight increase in the *preferred* population firing rate for the only top-down case, which follows the slight increase in the population-averaged rates of the sensory circuit due to the presence of feedback connections. In the sensory circuit, the differences in population rates are most noticeable at the beginning of the trial, for the only bottom-up case; and at the end of the trial for the only top-down case.

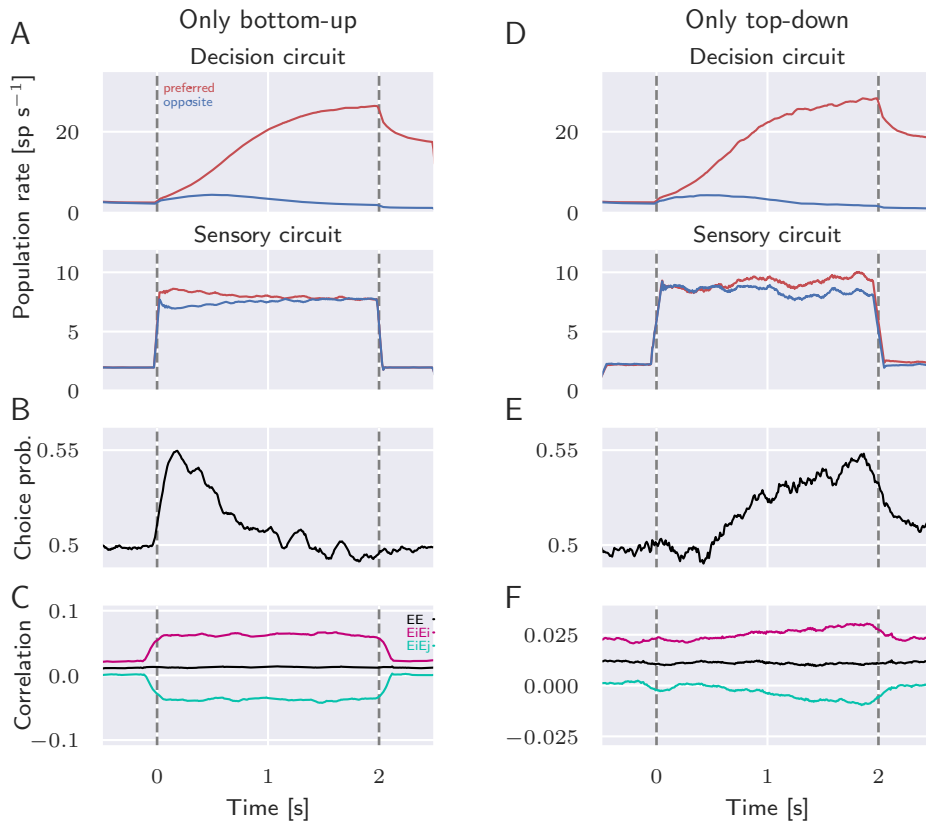


FIGURE 3.2: Bottom-up and top-down influences on choice probability exhibit different temporal dynamics. Hierarchical network with only bottom-up connections (A-C, $b_{FB}=0$), and with only top-down connections (D-F, through replicated stimuli and $b_{FB}=1$). (A, D) Average population rates for decision and sensory circuits. (B, E) Instantaneous averaged CP and (C, F) spike count noise correlations from 100 randomly selected excitatory sensory neurons.

Instantaneous CP traces show an early bottom-up component, which decays after one second from the stimulus onset (Figure 3.2B); and a late top-down component, which slowly ramps up until the stimulus offset (Figure 3.2E). The magnitude of the traces (~ 0.55) are comparable to the original results on the hierarchical network and thus, to the experimental measurements.

The time-course of correlations (Figure 3.2C, F) between pairs of sensory excitatory neurons support the notion that neurons within the same population (E_iE_i , magenta traces) exhibit positive correlations, whereas neurons across populations (E_iE_j , cyan traces) show negative correlations. Positive and negative correlations cancel out when computing the overall correlations between all pairs of neurons (EE , black traces). However, the cancellation is not total, because overall correlations are slightly positive (~ 0.0125) due to shared background activity. In the only bottom-up case (Figure 3.2C), correlations are sustained throughout the stimulus presentation. In the only top-down case (Figure 3.2F), correlations ramp up following top-down feedback inputs. Top-down correlations are lower in magnitude

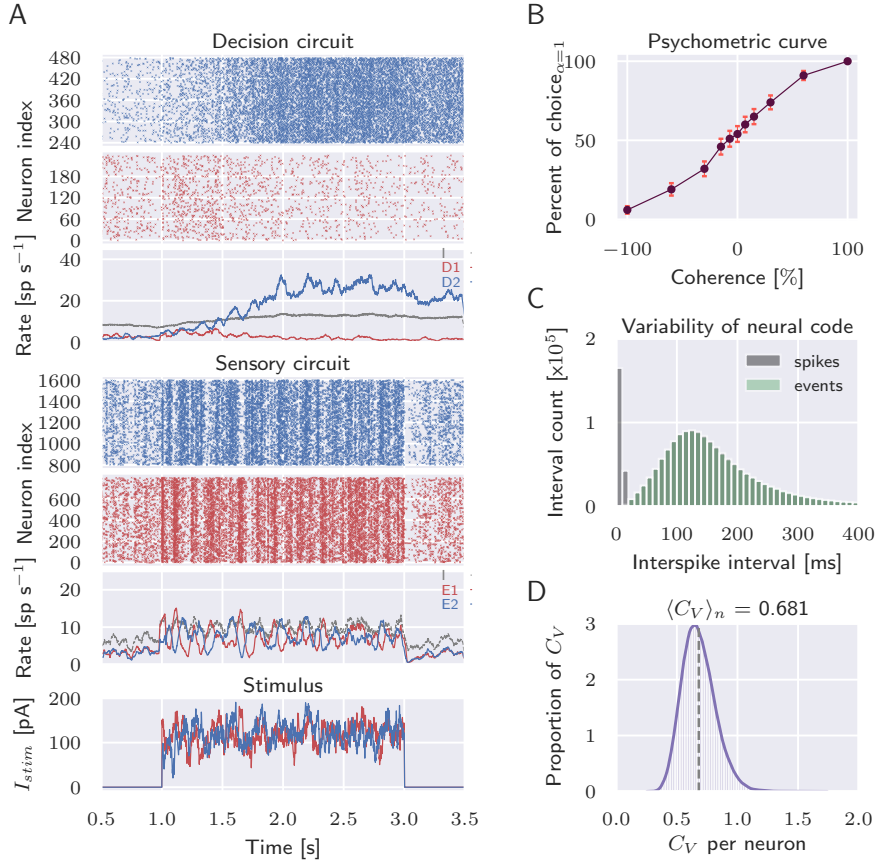


FIGURE 3.3: Replacement of sensory neurons changes the behavior of the hierarchical network. (A-D) Same as in Figure 3.1.

(~ 0.03) than those elicited by bottom-up fluctuations (~ 0.06), because top-down inputs are weaker than external stimuli to the sensory circuit.

3.2 Hierarchical network with two-compartment sensory neurons

The following section shows the results of the hierarchical network after the replacement of sensory excitatory neurons by two-compartment L5 pyramidal neurons.

3.2.1 Two-compartment sensory neurons affect bottom-up influences on choices

A single simulated trial of the hierarchical network with two-compartment sensory neurons is shown in Figure 3.3A. The network architecture is the same, except for

the re-wiring of top-down connections to the dendritic compartment of L5 pyramidal neurons. For this network, the stimulus input currents have a mean $I_0=120$ pA (Figure 3.3A, bottom panel). Excitatory populations E1 and E2 in the sensory circuit (A, middle panels) still track fluctuations in the stimulus, but now the *winner* population dominates over the *opposite* one with shorter intervals (red and blue traces). The inhibitory population (gray trace) still exhibits an overall higher firing rate than the excitatory populations. After stimulus offset, E1 and E2 are silenced due to the intrinsic inhibition led by the adaptation variable, a characteristic not seen in the original hierarchical network.

In Figure 3.3B, the psychometric curve shows that the introduction of L5 pyramidal neurons affects the performance of the network. The relationship becomes less sigmoidal and as a consequence the networks fails to represent a classical perception task. Moreover, at zero-coherent stimuli the network presents a slight bias towards the choice $\alpha=1$, which represents the stimulus-selective population D1.

The inter-spike interval (ISI) distribution (Figure 3.3C) indicates that spiking in L5 pyramidal neurons is still Poisson-like. However, now the mean ISI is longer (100-120 ms), when disregarding the shortest (0-20 ms) intervals. Furthermore, the spikes and events distribution perfectly overlap except for short intervals under 0-20 ms. Overall, the sensory circuit with two-compartmental L5 pyramidal neurons presents more bursting than the original sensory circuit (average burst size is 3.1 spikes per burst, average burst fraction $F \sim 15\%$, data not shown).

L5 pyramidal neurons present a mean $C_V=0.681$ (Figure 3.3D), indicating more regular spiking patterns. However, neurons with intrinsic bursting tend to exhibit more variable spiking patterns (i.e., $C_V>1$). The two-compartment L5 pyramidal neurons indeed contain an intrinsic burst mechanism, but somatic spiking is limited by the adaptation variable $w^{(s)}$, which injects a decaying negative current (controlled by parameter $b_w^{(s)}=-200$ pA, see Table 3.1) to the soma whenever a spike was present.

A comparison between the original hierarchical network and the hierarchical network with two-compartment sensory neurons is shown in (Figure 3.4). Population-averaged firing rates for the decision and sensory circuits are shown in Figure 3.4A, D. The behavior of the decision circuit is similar in both networks, except for a noticeable difference between the *preferred* and *opposite* populations as early as stimulus onset in the case of two-compartment sensory neurons. On the other hand, the sensory circuit shows tremendously different dynamics between both networks. The initial firing rate is higher in the two-compartment sensory neurons (> 10 sp s $^{-1}$), and stabilizes shortly after 100 ms of stimulus onset.

Interestingly, bottom-up influences on CP disappear in the network with two-compartment sensory neurons (Figure 3.4E), while pair noise correlations exhibit similar time-courses to the original hierarchical network with lower amplitudes (Figure 3.4F). The latter observations are indicative of a reduction in the fluctuations

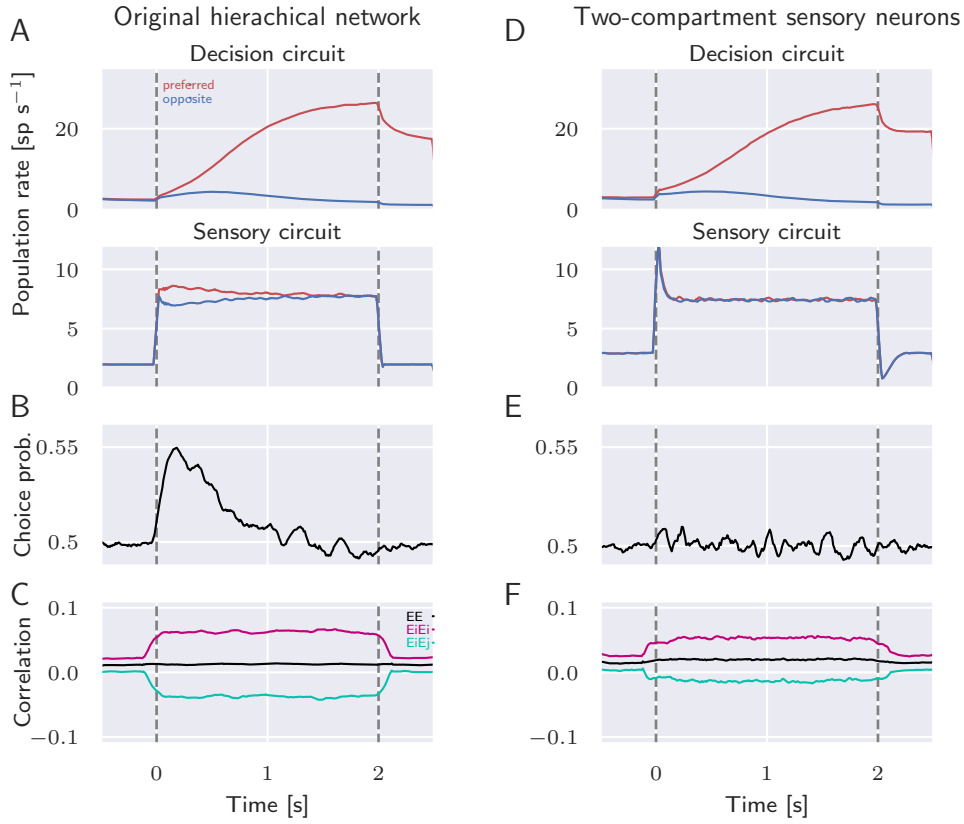


FIGURE 3.4: Bottom-up influences on CP disappear in the hierarchical network with two-compartment sensory neurons. Original hierarchical network with only bottom-up connections (A-C, $b_{FB}=0$, same as in Figure 3.2A-C), and hierarchical network with two-compartment sensory neurons and only bottom-up connections (D-F, $b_{FB}=0$). (A, D) Average population rates for decision and sensory circuits. (B, E) Instantaneous average CP and (C, F) spike count noise correlations.

from external stimuli (Churchland et al. 2010). The somatic spike-triggered adaptation $w^{(s)}$ is one main difference between the sensory neural models, and may reduce the fast fluctuations in the external stimulus given low-pass filtering properties.

Overall, this section shows how two-compartment sensory neurons differently affect upcoming decisions in comparison with the original sensory neurons. Both the spiking variability in the sensory circuit and the lack of a bottom-up component of CP, highlight that the different behavior may be related to somatic spike-triggered adaptation. Thus, I next explored the behavior of L5 pyramidal neurons without somatic adaptation.

3.2.2 Extended hierarchical network models perceptual decisions

L5 pyramidal neurons without spike-triggered adaptation and the parameter setup described in Table 3.1, cease to interfere with the hierarchical network's behavior

	HN	2c	EHN	
$C_m^{(s)}$	250	370	370	pF
$\tau_m^{(s)}$	15	16	16	ms
τ_{ref}	2	3	3	ms
E_{inh}	-80	-70	-80	mV
$a_w^{(d)}$	-	-13	-30	pA
$b_w^{(s)}$	-	-200	0	pA
$\bar{g}_{\text{I},\text{GABA}_A}$	1.52	-	2	nS
I_0	80	120	175	pA
b_{FB}	1	-	20	-
$\sim \bar{I}_{\text{E},\text{AMPA}}^{(d)}$	-	400	200	pA

TABLE 3.1: Parameter values used in the simulations. HN refers to the parameters for sensory excitatory neurons in the original hierarchical network described in Wimmer et al. (2015). 2c refers to the original two-compartment model for L5 pyramidal neurons described in Naud and Sprekeler (2018). EHN is the parameter setup proposed in this thesis because it enables intrinsic bursting while maintaining the properties of the hierarchical network.

(Figure 3.5). For the purposes of this work, the hierarchical network with these parameter setting is termed *extended* hierarchical network (EHN).

The psychometric curve (Figure 3.5A) shows an unbiased network (i.e., the network performance for zero-coherent stimuli is at chance level) capable of representing a perceptual task (i.e., it follows a sigmoidal shape). The average ISI for L5 pyramidal neurons (Figure 3.5B) is again short (between 0-20 ms), and the mean C_V becomes more regular (1.024, Figure 3.5C). The latter indicates that these neurons present Poisson-like firing with a strong presence of bursts (average burst size is 2.8 spikes per burst, average burst fraction $F \sim 15\%$, data not shown). Moreover, L5 pyramidal neurons elicit $\sim 10\%$ less amount of spikes than the original sensory excitatory neurons (from 16.6×10^5 to 14.9×10^5 spikes in 1000 trials).

To summarize, the EHN version of two-compartment L5 pyramidal neurons combines both the spiking variability observed in the original excitatory sensory neurons and the bursting activity observed in L5 pyramidal neurons.

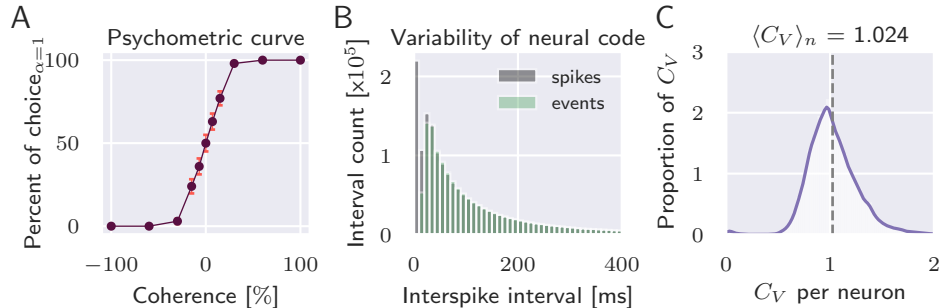


FIGURE 3.5: L5 pyramidal neurons without somatic adaptation reproduce hierarchical network's behavior. (A-C) Same as in Figure 3.1B-D and 3.3B-D.

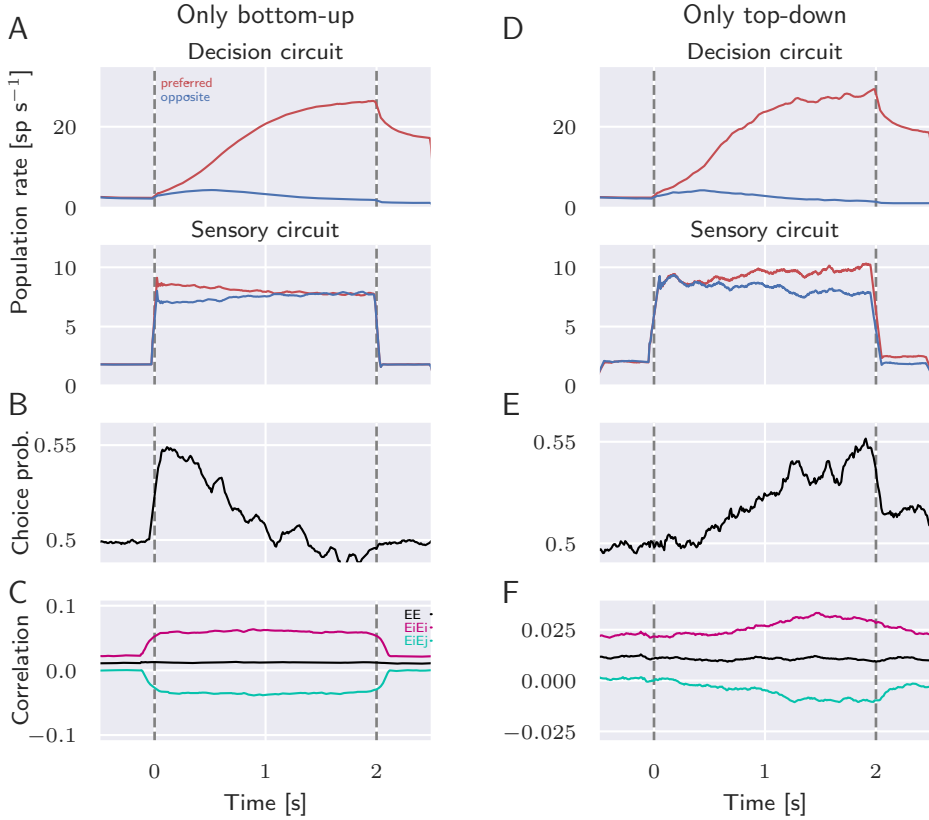


FIGURE 3.6: Extended hierarchical network reproduces bottom-up and top-down influences on choice probability. (A-F) Same as in Figure 3.2, except that $b_{FB}=20$ for the only top-down condition.

The extended hierarchical network successfully reproduces the results regarding the influences on CP (Figure 3.6). By systematically isolating the bottom-up and top-down contributions to neuronal variability in the sensory circuit, the respective early (Figure 3.6B) and late (Figure 3.6E) influences on CP are observed in the extended network. For the only top-down case, the feedback amplification variable $b_{FB}=20$ leads to an equivalent response to the weak top-down inputs ($b_{FB}=1$) observed in the original hierarchical network (see Table 3.1).

Average firing rates for the *preferred* and *opposite* populations (Figure 3.6A, D) exhibit similar dynamics and magnitudes to the original network ($\sim 30 \text{ sp s}^{-1}$ for the decision circuit and $\sim 10 \text{ sp s}^{-1}$ for the sensory circuit). Pair noise correlations (Figure 3.6C, F) between L5 pyramidal neurons also follow similar dynamics and magnitudes to the original network.

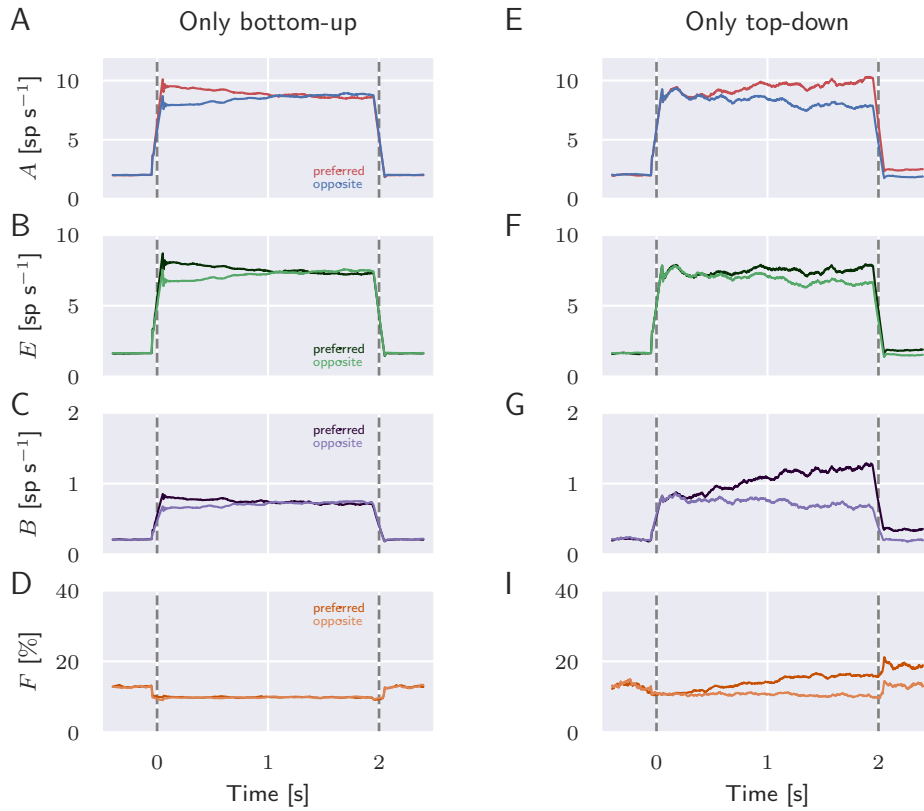


FIGURE 3.7: Averaged burst fraction from sensory neurons represents the top-down stream of information. Network with only bottom-up connections (A-D, $b_{FB}=0$), and with only top-down connections (E-I, through replicated stimuli). Neurometric analysis on a group of 100 randomly selected sensory neurons outputs the population average firing rate A (A, E, see Figure 3.6), event rate E (B, F), burst rate B (C, G) and burst probability F (D, I) for the *preferred* and *opposite* populations.

3.3 Decoding top-down influence through a multiplexed neural code

The neurometric analysis on the extended hierarchical network (Figure 3.7) confirms a distinction in the neural code for the two streams of information. First, the averaged firing rates A from 100 active L5 pyramidal neurons (Figure 3.7A, E) closely represents the population-averaged firing rates of the sensory circuit in both connectivity cases in Figure 3.6A,D. Firing rate A for the *preferred* subpopulation is higher shortly after stimulus onset and then decays in the only bottom-up case (Figure 3.7A), whereas it ramps up to a maximum towards the late stage of stimulus presentation in the only top-down case (Figure 3.7E). Event rates E of *preferred* and *opposite* populations (Figure 3.7B, F) show similar time-courses to A , but smaller in amplitude ($\sim 7.5 \text{ sp s}^{-1}$ vs $\sim 10 \text{ sp s}^{-1}$).

The burst rate B of the *preferred* population shows a minimal increase at the beginning of the trial in the network with only bottom-up connections (Figure 3.7C),

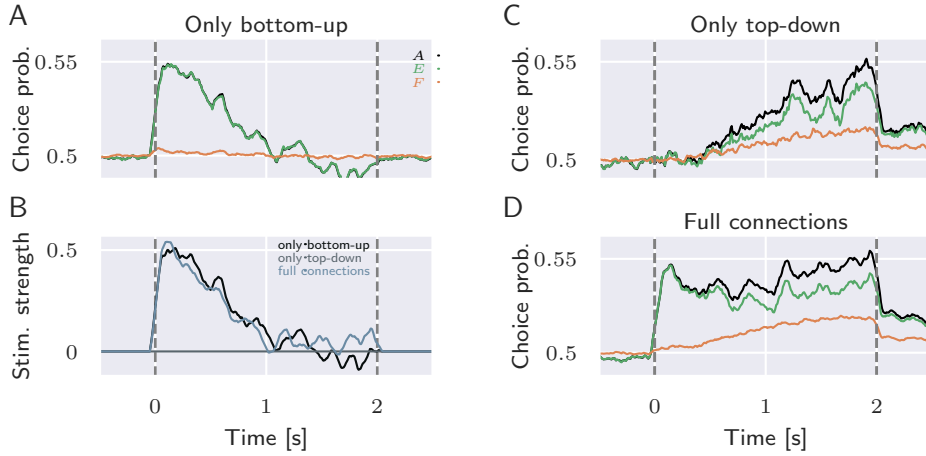


FIGURE 3.8: Averaged burst fraction directly decodes top-down influence on CP in a fully-connected network. CP from sensory neurons in the extended hierarchical network with only-bottom (A), only top-down (C) and full connections (D). Different traces represent the neural code used to calculate CP: firing rate A in black, event rate E in green and burst fraction F in orange. (B) Psychophysical kernel for the three connectivity cases of the hierarchical network: only bottom-up connections (black), only top-down connections (gray) and both bottom-up and top-down connections (light blue).

and a stronger, slowly building increase at the end of the trial in the network with only top-down connections (Figure 3.7G). The burst fraction F in the only top-down case (Figure 3.7I), follows similar dynamics described in the other neurometric measurements: the *preferred* population exhibits a slowly building increase from 10% at stimulus onset, to \sim 20% at stimulus offset; whereas the *opposite* population remains unchanged. Notably, burst fraction dynamics in the network with only bottom-up connections (Figure 3.7D) no longer exhibit a difference between populations at the beginning of the trial. Thus, top-down inputs to L5 pyramidal neurons are encoded in the population-averaged burst fraction F in the extended hierarchical network. Interestingly, bottom-up inputs can not be isolated through the population-averaged event rate E (i.e., they encode information when only top-down connections are present).

If different neural codes transmit the bottom-up and top-down streams of information at a population level, it may be possible to extract the corresponding bottom-up and top-down influences on CP using E and F respectively, by averaging over multiple trials of a single neuron. Consequently, CP was calculated from the different neural codes found in L5 pyramidal neurons: CP_E refers to CP from single neuron event counts E and CP_F , to CP from the burst fraction of single neurons (Figure 3.8). CP from the normal firing rate A represents the same traces as in Figure 3.6B, E.

In the network with only bottom-up connections (Figure 3.8A), the averaged time-course of CP from the normal firing rate A (black trace) exactly overlaps with

the CP_E (green trace). In contrast, CP_F (orange trace) remains unchanged throughout the stimulus presentation. Thus, the information encoded in F does not contribute to the upcoming choice when the network lacks top-down connections. If we recall the theory behind multiplexing in L5 pyramidal neurons (Naud and Sprekeler 2018), this is an expected result because F mainly reflects the top-down stream of information.

The psychophysical kernel, which indicates when stimulus fluctuations influence behavior the most (Nienborg and Cumming 2009), is shown in (Figure 3.8B). For the only bottom-up case (black trace), the time-course peaks early and decreases as the experiment unfolds, exactly matching CP traces from A and E in Figure 3.8A. This result indicates that sensory evidence mostly influences decisions shortly after a stimulus is presented, even in the presence of feedback connections (light blue trace), and supports the results of Wimmer et al. (2015). In contrast, sensory evidence does not contribute to the upcoming choice when the network only has top-down connections. This is clear if we recall that the only top-down case is achieved through the presentation of replicated stimuli.

The result of calculating CP from different neural codes in the top-down case is shown in Figure 3.8C. CP_E (green trace) closely follows that from the normal firing rate A (black trace), instead of exactly matching it. Interestingly, the difference between both traces increases towards the end of the trial. On the other hand, CP_F (orange trace), slowly ramps as the experiment unfolds following CP from A . Remarkably, the difference between CP from A and F decreases as the experiment unfolds, reaching a minimum at stimulus offset. This result shows two important observations:

1. Top-down influence on CP is maximal at stimulus offset and it can be directly calculated from the burst fraction F of single L5 pyramidal neurons.
2. CP_E of single L5 pyramidal neurons reflects top-down information. However, the overall amplitude of CP_E decreases as the information encoded in F increases.

Finally, the calculation of CP from different neural codes in a fully connected hierarchical network (i.e., with both bottom-up and top-down connections) is shown in (Figure 3.8D). Surprisingly, the top-down influence is robustly represented in the CP calculated from F (orange trace): ramps up towards a maximum at the stimulus offset. Moreover, the bottom-up influence is fully encoded by CP from E (green trace) at the beginning of the trial. Again, as the experiment unfolds we see that the magnitude of CP from E decreases, which is in agreement with the early, decaying bottom-up component of CP revealed by Wimmer et al. (2015). These results prove that the bottom-up and top-down influences on CP can be extracted directly from the event rate (E) and burst fraction (F) of single L5 pyramidal neurons in normal experimental conditions.

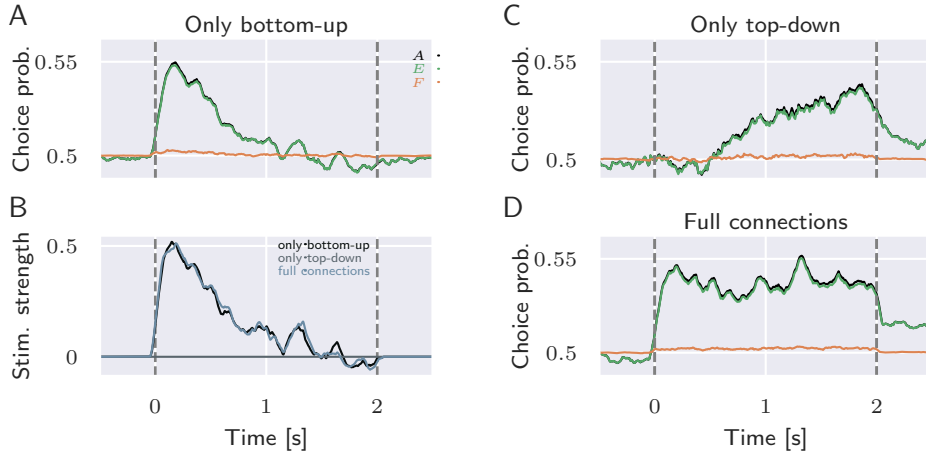


FIGURE 3.9: Averaged burst fraction fails to decode top-down influence on CP in the original hierarchical network. (A-D) Same as in Figure 3.8.

As a control case, the same neurometric analysis was used in the original hierarchical network (Figure 3.9). It is necessary to evaluate to what extend the event rate E and burst fraction F represent the two information streams in a model without intrinsic bursting. The only bottom-up case is exactly the same as with the extended hierarchical network (Figure 3.8A), because of the lack of top-down inputs and thus, the absent role of dendrites. The psychophysical kernel (Figure 3.8B) also yields analogous results, because the stimuli used are modeled in the same way. However, in the only top-down case (Figure 3.8C) and in the fully-connected network (Figure 3.8D), CP from the burst fraction F is not informative. Thus, in a model without a dendritic compartment and without intrinsic bursting, the neural code fails to separate the two streams of information.

Chapter 4

Discussion

Choice probability encompasses the relationship between sensory neural activity and upcoming decisions. Since the first description of this phenomenon by Britten et al. (1996), various experimental studies have validated the role of sensory neurons on behavioral choices during perceptual tasks. However, the interpretation of this role remained unclear until recently. Using sophisticated computational modeling, Wimmer et al. (2015) suggest that early in the perceptual task, bottom-up fluctuations causally influence upcoming decisions, and then top-down influences take over. In this project, I proposed a direct and generalizable method to clarify the interpretation of CP by distinguishing different neural codes in the spiking patterns of sensory neurons.

The first task included the development of a replica of the hierarchical network model for perceptual decision making proposed by Wimmer et al. (2015). The model performs a two-choice RDM perceptual task using an extension of the canonical neurobiological model of decision making by Wang (2002). Specifically, their extension included sensory neurons that relay external stimulus information to the decision circuit, while also receiving feedback connections from the decision circuit. This way, bottom-up and top-down contributions to the activity of sensory neurons were isolated. Moreover, the relationship between sensory neuronal activity and upcoming decisions was disentangled into an early, bottom-up and a late, top-down contribution on choice.

The second task involved the replacement of sensory neurons in the hierarchical network by two-compartment L5 pyramidal neurons until achieving a stable model for perceptual decision making. A *naive* replacement of the sensory units led to a failure in the representation of perceptual decisions. Specifically, L5 pyramidal neurons exhibited different variability in the neural code than that presented in the sensory neurons of the original hierarchical network. Most importantly, the hierarchical network with the *naive* replacement failed to elicit the bottom-up contribution on CP. An in-depth assessment showed that the spike-triggered adaptation ($w^{(s)}$) included in the soma of the two-compartment L5 pyramidal neurons, was responsible for the most noticeable changes. After removing the somatic adaptation variable $w^{(s)}$, L5 pyramidal neurons maintained their bursting capacity and the extended hierarchical network adequately represented perceptual decisions (Figure 3.5).

Finally, the third task evaluated the multiplexing capacity of L5 pyramidal neurons within the extended hierarchical network. According to Naud and Sprekeler (2018), the event rate E of a population of L5 pyramidal neurons mostly tracks the bottom-up information stream, whereas its burst fraction F represents the top-down information stream. Once the extended hierarchical network successfully reproduced perceptual decisions, the influences underlying CP were directly assessed through the neurometric analysis. In a fully-connected network, the top-down influence on CP was successfully encoded in the averaged burst fraction F of single L5 pyramidal neurons. Whereas the bottom-up influence on CP was embedded in the averaged event rate E of L5 pyramidal neurons. However, the signal was not completely isolated, because there was cross-talk with the recurrent information reverberating in the sensory circuit.

4.1 Stabilization of hierarchical network with two-compartment sensory neurons

The intrinsic bursting mechanism of L5 pyramidal neurons enables high-frequency firing as soon the external stimulus is delivered (Figures 3.3 and 3.4). This sudden change in the somatic firing rate of sensory neurons recruits strong inhibition through the spike-triggered adaptation variable $w^{(s)}$.

In this work, I showed how the somatic adaptation variable $w^{(s)}$ changed the hierarchical network's behavior (Section 3.2.1). In general, sensory neurons present noticeable responses to sensory stimuli, but after a prolonged presentation of the stimulus neurons adapt by eliciting reduced responses or prolonged inter-spike-intervals. Adaptation in neurons is known to be an efficient way of transmitting information, but also results in an ambiguity of the neural code. The problem is that the same stimulus will have different responses once adaptation has entered the equation, and the variability of external evidence will be lost. There are models that solve the ambiguity of adaptive populations of neurons (Naud and Gerstner 2012), but for the present work the hierarchical network's findings were best reproduced using sensory pyramidal neurons without spike-triggered adaptation.

The somatic adaptation variable $w^{(s)}$ was also responsible for a loss in the bottom-up influence on CP (Figure 3.4). The spike-triggered adaptation variable introduces regularity in the spiking patterns of two-compartment sensory neurons and acts as a low-pass filter of the external stimuli. Thus, fluctuations on sensory neuronal activity after stimuli onset were diminished and the contribution of an early component on CP was abolished.

Last, I showed how strong bursting in the sensory population promptly influences stimulus-selective populations D1 and D2 in the decision circuit. This leads to a difference in the *preferred* and *opposite* population rates immediately after stimulus onset (Figure 3.4). In order to maintain the original network's dynamics, the sensory circuit with two-compartment neurons (see Table 3.1) also demanded higher

inhibitory recurrent synaptic contributions ($\bar{g}_{I,GABA_A}$ from 1.52 to 2 nS) and stronger dendritic adaptation ($a_w^{(d)}$ from -13 to -30 pA).

The increase in inhibitory feedback is related to the strong coupling between excitatory and inhibitory neurons in the sensory circuit. Given the strength and density of the connections in the sensory circuit, even small random fluctuations in excitatory neurons are sufficient to recruit inhibitory feedback (Renart et al. 2010). With two-compartment sensory neurons capable of bursting, the same external stimuli elicited more random fluctuations and thus, a stronger inhibitory feedback was needed to stabilize the circuit.

The stronger dendritic adaptation follows the idea of enabling efficient information transmission through bursting in a model without spike-triggered adaptation. If burst length is shorter (from an average 3.1 to 2.8 spikes per burst), the same information will be transmitted with less energy expenditure for generating spikes. At the same time, a stronger dendritic adaptation alleviates the sudden and strong influence in the decision populations dynamics after stimulus onset, because less bursts are produced.

4.2 Multiplexing in recurrent networks

L5 pyramidal sensory neurons in the extended hierarchical network show remarkable results regarding multiplexing (Figures 3.7 and 3.8). The burst fraction F fully represents the top-down information stream, and acts as a direct decoder of the top-down influences on CP during the two-choice RDM task. On the other hand, the event rate E does represent the bottom-up information stream, but includes cross-talk from the top-down stream through the reverberation of recurrent activity.

According to the theory of multiplexing, L5 pyramidal neurons are capable to represent two information streams through different neural codes in a network without recurrent connections (Naud and Sprekeler 2018). Thus, one possible answer to the different results presented in this work and the ones in Naud and Sprekeler (2018) could be related to the recurrent connections of the sensory circuit. In the hierarchical network for perceptual decision making, the recurrent connections are crucial for the network dynamics: they enable a tight-balance between excitatory and inhibitory neurons and are the underlying basis of correlated activity (Wimmer et al. 2015; Renart et al. 2010). However, a recurrent setup also enables the combination of the bottom-up and the top-down streams of information in the somatic input. The propagation of dendritic inputs to the somatic input is done through the excitatory recurrent connections, which include the top-down information capable to elicit dendritic activity. Thus, the multiplexing property of L5 pyramidal neurons is difficult to achieve if the neurons are part of a circuit with recurrent connections.

A possible solution to prevent the propagation of dendritic inputs could be to include top-down connections to the inhibitory population. In this setup, sensory pyramidal neurons could differentiate between bottom-up and top-down inputs

through recurrent inhibition. This idea is derived from experimental reports in sensory cortex, in which both excitatory and inhibitory neurons receive top-down inputs (D’Souza and Burkhalter 2017) and are equally selective for particular stimuli during decision making (Najafi et al. 2018). However, appropriately simulations still need to be conducted in order to assess the validity of the proposition.

4.3 Future perspectives

One of the major challenges regarding the study of decision making is to address the diverse set of biases in individuals according to specific conditions (Linares, Aguilar-Lleyda, and López-Moliner 2019). In perceptual decision making this challenge can be tackle by studying different decision networks, with various initial conditions across multiple perceptual tasks. In this work, the stable implementations of the original and extended hierarchical networks for perceptual decision making were possible given the use of a specific connectivity matrix for each case. Interestingly, certain connectivity matrices lead to inherent choice biases and thus, to biased representations of the two RDM task. Wimmer et al. (2015) also reported a similar issue and indicated without concrete results that the same bottom-up and top-down contributions on CP are found in any hierarchical network. In order to accurately study perceptual decisions under various conditions, a generalization of the results pertaining the hierarchical network is needed. However, this is not possible using networks with fixed connectivity matrices.

If intrinsic biases affect the psychometric curves of decision networks, then it is possible that they can also affect the underlying mechanisms of CP. The problem regarding intrinsic biases is again related to the nature of the bias, which is difficult to clarify. How can we know if decisions are being influenced by sensory biases or choice biases? And furthermore, is the bias encompassing a pre-decision or a post-decision signal? A top-down signal can bias perceptual decisions even before evidence is presented, if expectation or the focus of attention is embedded in them (Cohen and Maunsell 2009; Rolls and Deco 2011). For example, this can be seen in a connectivity biased network, in which the sensory evidence is completely disregarded. On the other hand, a pure post-decision signal will only reflect the representation of the chosen percept (Nienborg and Cumming 2009), and an assessment of the nature of bias in the network would be difficult. The latter is the case of the hierarchical network, because recurrent, feed-forward and feed-back connections are active before, during and after stimulus presentation. Overall, the recognition of top-down signal as purely post-decisions is a complicated matter.

In the field of perceptual decision making, there are various techniques to reveal the bottom-up influence of sensory neurons to behavioral choices. For example, using the reverse correlation technique to obtain the psychophysical kernel of a decision making task (Gerstner et al. 2014). Hitherto, the major unresolved problem is to pinpoint the top-down influence in the activity of sensory neurons during

perceptual decisions (Urai and Murphy 2016). The results of the present thesis aim to give an alternative solution to the specific recognition of the top-down contribution on CP. A neurometric analysis of various decision networks under a diverse set of conditions could solve the ambiguity of the underlying components behind the variability in sensory neuronal responses and their relationship to upcoming decisions. Furthermore, because the method relies on the distinction between different spiking patterns, it can also be corroborated using actual experimental recordings. Overall, the present work suggests a simple and generalizable approach that bridges biophysical principles and cognitive behavior, and exploits the decoding properties embedded in the different neural codes present in sensory neurons.

Bibliography

- Britten, K. H. et al. (1996). "A relationship between behavioral choice and the visual responses of neurons in macaque MT". In: *Visual Neuroscience* 13.1, pp. 87–100. DOI: [10.1017/S095252380000715X](https://doi.org/10.1017/S095252380000715X).
- Churchland, Mark M et al. (2010). "Stimulus onset quenches neural variability: a widespread cortical phenomenon". In: *Nature Neuroscience* 13.3, pp. 369–378. DOI: [10.1038/nn.2501](https://doi.org/10.1038/nn.2501).
- Cohen, Marlene R. and John H R Maunsell (2009). "Attention improves performance primarily by reducing interneuronal correlations". In: *Nature Neuroscience* 12.12, pp. 1594–1600. DOI: [10.1038/nn.2439](https://doi.org/10.1038/nn.2439).
- Crapse, Trinity B. and Michele A. Basso (2015). "Insights into decision making using choice probability". In: *Journal of Neurophysiology* 114.6, pp. 3039–3049. DOI: [10.1152/jn.00335.2015](https://doi.org/10.1152/jn.00335.2015).
- Cumming, Bruce G and Hendrikje Nienborg (2016). "Feedforward and feedback sources of choice probability in neural population responses". In: *Current Opinion in Neurobiology* 37, pp. 126–132. DOI: [10.1016/j.conb.2016.01.009](https://doi.org/10.1016/j.conb.2016.01.009).
- D'Souza, Rinaldo D. and Andreas Burkhalter (2017). "A Laminar Organization for Selective Cortico-Cortical Communication". In: *Frontiers in Neuroanatomy* 11, p. 71. DOI: [10.3389/fnana.2017.00071](https://doi.org/10.3389/fnana.2017.00071).
- Gerstner, Wulfram et al. (2014). *Neuronal Dynamics: From Single Neurons to Networks and Models of Cognition*. Cambridge, United Kingdom: Cambridge University Press.
- Gold, Joshua I. and Michael N. Shadlen (2007). "The Neural Basis of Decision Making". In: *Annual Review of Neuroscience* 30.1, pp. 535–574. DOI: [10.1146/annurev.neuro.29.051605.113038](https://doi.org/10.1146/annurev.neuro.29.051605.113038).
- Haefner, Ralf M et al. (2013). "Inferring decoding strategies from choice probabilities in the presence of correlated variability". In: *Nature Neuroscience* 16.2, pp. 235–242. DOI: [10.1038/nn.3309](https://doi.org/10.1038/nn.3309).
- Larkum, Matthew (2013). "A cellular mechanism for cortical associations: an organizing principle for the cerebral cortex". In: *Trends in Neurosciences* 36.3, pp. 141–151. DOI: [10.1016/j.tins.2012.11.006](https://doi.org/10.1016/j.tins.2012.11.006).
- Larkum, Matthew E., J. Julius Zhu, and Bert Sakmann (1999). "A new cellular mechanism for coupling inputs arriving at different cortical layers". In: *Nature* 398.6725, p. 338. DOI: [10.1038/18686](https://doi.org/10.1038/18686).

- Linares, Daniel, David Aguilar-Lleyda, and Joan López-Moliner (2019). "Decoupling sensory from decisional choice biases in perceptual decision making". In: *eLife* 8.e43994, p. 16.
- Machens, Christian K., Ranulfo Romo, and Carlos D. Brody (2005). "Flexible Control of Mutual Inhibition: A Neural Model of Two-Interval Discrimination". In: *Science* 307.5712, pp. 1121–1124. DOI: [10.1126/science.1104171](https://doi.org/10.1126/science.1104171).
- Major, Guy, Matthew E. Larkum, and Jackie Schiller (2013). "Active Properties of Neocortical Pyramidal Neuron Dendrites". In: *Annual Review of Neuroscience* 36.1, pp. 1–24. DOI: [10.1146/annurev-neuro-062111-150343](https://doi.org/10.1146/annurev-neuro-062111-150343).
- Manita, Satoshi et al. (2017). "Dendritic Spikes in Sensory Perception". In: *Frontiers in Cellular Neuroscience* 11. DOI: [10.3389/fncel.2017.00029](https://doi.org/10.3389/fncel.2017.00029).
- Najafi, Farzaneh and Anne K. Churchland (2018). "Perceptual Decision-Making: A Field in the Midst of a Transformation". In: *Neuron* 100.2, pp. 453–462. DOI: [10.1016/j.neuron.2018.10.017](https://doi.org/10.1016/j.neuron.2018.10.017).
- Najafi, Farzaneh et al. (2018). *Excitatory and inhibitory subnetworks are equally selective during decision-making and emerge simultaneously during learning*. Preprint. Neuroscience. DOI: [10.1101/354340](https://doi.org/10.1101/354340).
- Naud, Richard and Wulfram Gerstner (2012). "Coding and Decoding with Adapting Neurons: A Population Approach to the Peri-Stimulus Time Histogram". In: *PLoS Computational Biology* 8.10. Ed. by Olaf Sporns, e1002711. DOI: [10.1371/journal.pcbi.1002711](https://doi.org/10.1371/journal.pcbi.1002711).
- Naud, Richard and Henning Sprekeler (2018). "Sparse bursts optimize information transmission in a multiplexed neural code". In: *Proceedings of the National Academy of Sciences* 115.27, E6329–E6338. DOI: [10.1073/pnas.1720995115](https://doi.org/10.1073/pnas.1720995115).
- Nienborg, Hendrikje and Bruce G. Cumming (2009). "Decision-related activity in sensory neurons reflects more than a neuron's causal effect". In: *Nature* 459.7243, pp. 89–92. DOI: [10.1038/nature07821](https://doi.org/10.1038/nature07821).
- Nienborg, Hendrikje, Marlene R. Cohen, and Bruce G. Cumming (2012). "Decision-Related Activity in Sensory Neurons: Correlations Among Neurons and with Behavior". In: *Annual Review of Neuroscience* 35.1, pp. 463–483. DOI: [10.1146/annurev-neuro-062111-150403](https://doi.org/10.1146/annurev-neuro-062111-150403).
- Parker, A. J. and W. T. Newsome (1998). "SENSE AND THE SINGLE NEURON: Probing the Physiology of Perception". In: *Annual Review of Neuroscience* 21.1, pp. 227–277. DOI: [10.1146/annurev.neuro.21.1.227](https://doi.org/10.1146/annurev.neuro.21.1.227).
- Renart, A. et al. (2010). "The Asynchronous State in Cortical Circuits". In: *Science* 327.5965, pp. 587–590. DOI: [10.1126/science.1179850](https://doi.org/10.1126/science.1179850).
- Resulaj, Arbora et al. (2009). "Changes of mind in decision-making". In: *Nature* 461.7261, pp. 263–266. DOI: [10.1038/nature08275](https://doi.org/10.1038/nature08275).
- Rolls, Edmund T. and Gustavo Deco (2011). "Prediction of Decisions from Noise in the Brain before the Evidence is Provided". In: *Frontiers in Neuroscience* 5. DOI: [10.3389/fnins.2011.00033](https://doi.org/10.3389/fnins.2011.00033).

- Romo, Ranulfo et al. (2002). "Neuronal correlates of decision-making in secondary somatosensory cortex". In: *Nature Neuroscience* 5.11, pp. 1217–1225. DOI: [10.1038/nn950](https://doi.org/10.1038/nn950).
- Shadlen, Mn et al. (1996). "A computational analysis of the relationship between neuronal and behavioral responses to visual motion". In: *The Journal of Neuroscience* 16.4, pp. 1486–1510. DOI: [10.1523/JNEUROSCI.16-04-01486.1996](https://doi.org/10.1523/JNEUROSCI.16-04-01486.1996).
- Stuart, Greg J. and Nelson Spruston (2015). "Dendritic integration: 60 years of progress". In: *Nature Neuroscience* 18.12, pp. 1713–1721. DOI: [10.1038/nn.4157](https://doi.org/10.1038/nn.4157).
- Urai, Anne E. and Peter R. Murphy (2016). "Commentary: Sensory integration dynamics in a hierarchical network explains choice probabilities in cortical area MT". In: *Frontiers in Systems Neuroscience* 10, p. 37. DOI: [10.3389/fnsys.2016.00037](https://doi.org/10.3389/fnsys.2016.00037).
- Wang, Xiao-Jing (2002). "Probabilistic Decision Making by Slow Reverberation in Cortical Circuits". In: *Neuron* 36.5, pp. 955–968. DOI: [10.1016/S0896-6273\(02\)01092-9](https://doi.org/10.1016/S0896-6273(02)01092-9).
- Wimmer, Klaus et al. (2015). "Sensory integration dynamics in a hierarchical network explains choice probabilities in cortical area MT". In: *Nature Communications* 6.1, p. 6177. DOI: [10.1038/ncomms7177](https://doi.org/10.1038/ncomms7177).